Journal of Clinical and Translational Hepatology **2024**
DOI: 10.14218/JCTH.2024.00375

Review Article

Fluorescence-guided Surgery for Hepatocellular Carcinoma: From Clinical Practice to Laboratories

Tian Xiao[1#], Didi Chen[2#], Li Peng[3], Zhuoxia Li[4], Wenming Pan[1], Yuping Dong[5], Jinxiang Zhang[1*] and Min Li[4*]

[1]Department of Emergency Surgery, Union Hospital, Tongji Medical College, Huazhong University of Science and Technology, Wuhan, Hubei, China; [2]Hubei Key Laboratory of Purification and Application of Plant Anti-Cancer Active Ingredients, Hubei University of Education, Wuhan, Hubei, China; [3]Department of Pathology, Union Hospital, Tongji Medical College, Huazhong University of Science and Technology, Wuhan, Hubei, China; [4]Department of Hepatobiliary Surgery, Union Hospital, Tongji Medical College, Huazhong University of Science and Technology, Wuhan, Hubei, China; [5]Beijing Key Laboratory of Construction Tailorable Advanced Functional Materials and Green Applications, School of Materials Science and Engineering, Beijing Institute of Technology, Beijing, China

Received: October 12, 2024 | **Revised:** December 06, 2024 | **Accepted:** December 12, 2024 | **Published online:** January 02, 2025

Abstract

Fluorescence navigation is a novel technique for accurately identifying hepatocellular carcinoma (HCC) lesions during hepatectomy, enabling real-time visualization. Indocyanine green-based fluorescence guidance has been commonly used to demarcate HCC lesion boundaries, but it cannot distinguish between benign and malignant liver tumors. This review focused on the clinical applications and limitations of indocyanine green, as well as recent advances in novel fluorescent probes for fluorescence-guided surgery of HCC. It covers traditional fluorescent imaging probes such as enzymes, reactive oxygen species, reactive sulfur species, and pH-sensitive probes, followed by an introduction to aggregation-induced emission probes. Aggregation-induced emission probes exhibit strong fluorescence, low background signals, excellent biocompatibility, and high photostability in the aggregate state, but show no fluorescence in dilute solutions. Design strategies for these probes may offer insights for developing novel fluorescent probes for the real-time identification and navigation of HCC during surgery.

Citation of this article: Xiao T, Chen D, Peng L, Li Z, Pan W, Dong Y, *et al*. Fluorescence-guided Surgery for Hepatocellular Carcinoma: From Clinical Practice to Laboratories. J Clin Transl Hepatol 2024. doi: 10.14218/JCTH.2024.00375.

Introduction

Hepatocellular carcinoma (HCC) is a significant public health concern worldwide. With over 780,000 cases diagnosed and more than 740,000 deaths each year, HCC is ranked as the sixth most common neoplasm and the third leading cause of cancer-related death.[1] Globally, the incidence and mortality rates of HCC are nearly equal, indicating poor treatment efficacy.[2] The majority of HCC cases occur in Eastern Asia and sub-Saharan Africa, where there is a high prevalence of hepatitis B virus infection[3] and many individuals are infected with the virus at birth.[4,5] Additionally, due to the increasing incidence of hepatitis C virus infection, the incidence of HCC is also rising in Western countries and Japan.[6] Other risk factors include heavy alcohol consumption, non-alcoholic fatty liver disease, obesity, and diabetes.[7–10] Certain genetic conditions, such as hemochromatosis, also increase the risk of HCC.[11]

Hepatectomy is one of the most effective treatments for HCC, and achieving radical resection of tumor lesions is critical for a successful outcome.[1,12] Otherwise, the presence of residual cancer cells after surgery can lead to cancer recurrence and poor prognosis. Therefore, surgeons rely on imaging technologies to locate the tumor lesion.[13] In the past several decades, imaging technologies such as computed tomography (CT), magnetic resonance imaging (MRI), and positron emission tomography have provided surgeons with valuable preoperative planning information for surgical procedures. However, real-time visualization of the tumor during surgery has been limited due to equipment constraints. Unlike these imaging technologies, intraoperative ultrasound (IOUS) can provide real-time feedback to identify the number and location of tumor lesions, guiding the surgical approach during the procedure.[14] However, there are several limitations to IOUS for HCC. Firstly, IOUS is highly dependent on the surgeon's skill level. Inexperienced surgeons may struggle to interpret the images and identify the tumor margins, which can result in incomplete tumor removal or damage to healthy liver tissue. Secondly, IOUS is a time-consuming procedure that can prolong surgery, increasing the risk of complications such as bleeding and infection. Thirdly, IOUS does not provide continuous real-time visualization because surgeons must perform intermittent ultrasonic detection during hepatectomy. In other words, the surgeon must transect the

Keywords: Hepatocellular carcinoma; Fluorescence-guided surgery; Fluorescent probes; Indocyanine green; Aggregation-induced emission luminogens; Surgical navigation.

[#]Contributed equally to this work.

[*]**Correspondence to:** Min Li, Department of Hepatobiliary Surgery, Union Hospital, Tongji Medical College, Huazhong University of Science and Technology, Wuhan, Hubei 430022, China. ORCID: https://orcid.org/0000-0002-0047-2804. E-mail: liminmed@hust.edu.cn; Jinxiang Zhang, Department of Emergency Surgery, Union Hospital, Tongji Medical College, Huazhong University of Science and Technology, Wuhan, Hubei 430022, China. ORCID: https://orcid.org/0000-0002-5447-272X. E-mail: zhangjinxiang@hust.edu.cn.

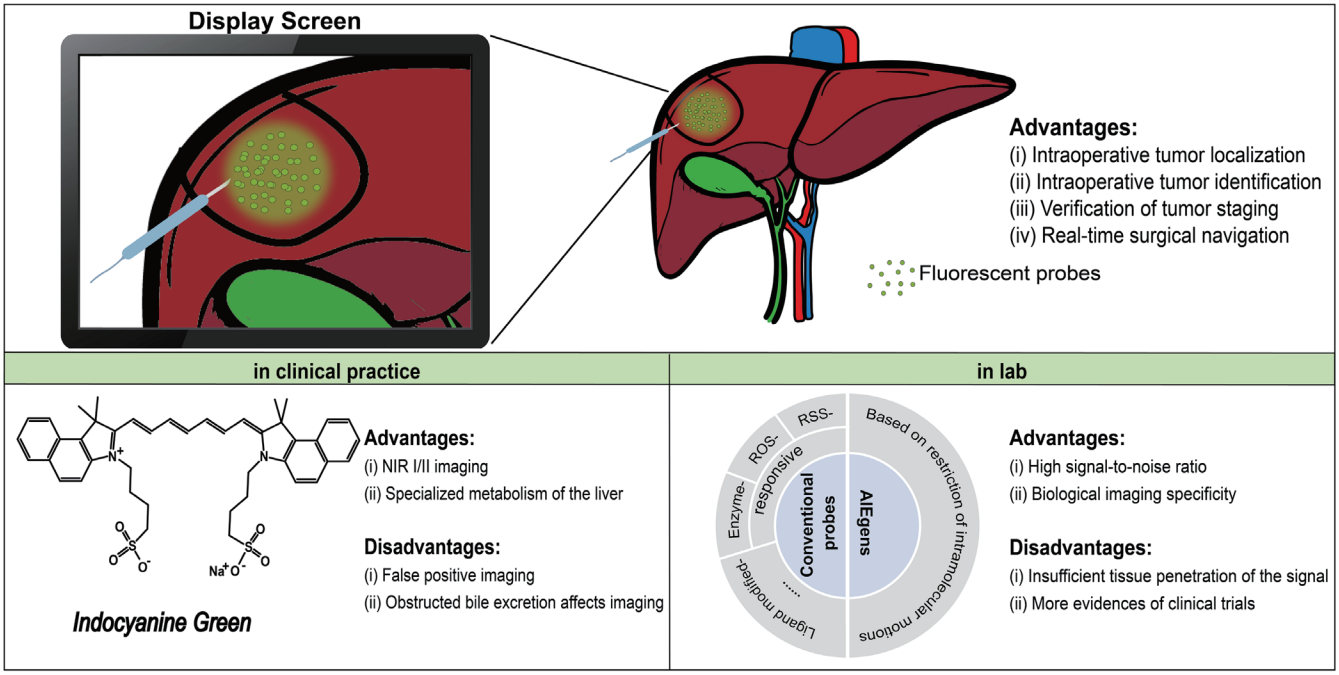

Scheme 1. Advantages and disadvantages of indocyanine green in clinical practice and new fluorescent probes in laboratory. NIR, Near infrared spectrum.

hepatic parenchyma after ultrasonic detection rather than under continuous ultrasonic monitoring.[15] For better surgical outcomes, the development of intraoperative imaging technology is a critical issue in liver resection for HCC.

In recent years, fluorescence-guided surgery (FGS) has gained attention as a novel technique that utilizes fluorescent dyes to highlight cancerous tissue during surgery, enabling more precise and thorough resection.[16–19] One of the main advantages of FGS in HCC surgery is its ability to differentiate between tumor and normal tissue with high sensitivity and specificity.[20] By administering a fluorescent dye that selectively accumulates in cancer cells, surgeons can visualize tumor borders and identify small satellite lesions that may otherwise go undetected. More importantly, the fusion image is displayed on a high-definition screen by integrating the fluorescent signal from the fluorescent dyes with standard unaided vision using white light imaging, thanks to advanced imaging system software. This allows surgeons to receive real-time guidance throughout the entire surgical procedure.[21]

In this review, we provide a summary of recent advances in fluorescent probes for the detection and treatment of HCC (Scheme 1). First, we introduce the commonly used fluorescence navigation methods in clinical practice. Next, we highlight the progress of novel fluorescent probes, which offer improved efficacy. Finally, we discuss the challenges and opportunities associated with using novel fluorescent probes in HCC surgery, with the goal of achieving more precise and thorough removal of cancerous tissue and improving overall survival rates.

Indocyanine green (ICG)-based FGS for HCC

ICG is currently the most widely used near-infrared (NIR) fluorescent dye certified by the US FDA, and it has been discovered and applied in clinical practice for nearly 60 years.[22] In recent years, due to the extensive development and application of new fluorescence imaging systems and fluorescence navigation equipment in clinical practice, ICG-based fluorescence imaging technology has rapidly advanced and gradually become more popular in China.[23] After intravenous injection, ICG binds to polymeric proteins such as albumin and lipoprotein in the plasma, where it neither undergoes metabolic breakdown nor alters the molecular structure of the bound protein, providing good intravascular stability. As ICG circulates through the blood vessels around the liver, it is actively transported and specifically taken up by liver cells. It is then secreted into the biliary system and eventually excreted into the intestine and eliminated from the body.[24] Normal liver tissue can completely clear ICG within 12–24 h, while ICG remains in tumor tissue for several weeks due to the impaired bile excretion function of liver cells in HCC tissue.[25] In practical applications, the complex biological environment can interfere with the fluorescence signal of probes. For example, experimental studies have shown that most of the light is absorbed and neutralized by hemoglobin (wavelengths less than 700 nm) and water (wavelengths greater than 900 nm) as fluorescent light penetrates biological tissues.[26] ICG molecules are excited by light with a wavelength of 750–810 nm and emit fluorescence with a peak wavelength of 840 nm, which falls within the "window" boundary (700–900 nm) of the deep red and NIR light spectrum, making it highly tissue-penetrating.[27] Under this optimal emission wavelength, the fluorescent signal from ICG can highlight tumor tissue, thus guiding the intraoperative resection of HCC.

In clinical practice, ICG-based FGS has been commonly utilized to identify and demarcate tumor boundaries at the cellular functional level due to the difference in excretion between HCC lesions and normal liver tissue.[28] With ICG injected intravenously several days before the operation, the tumor boundary can be delineated using ICG fluorescence detection during surgery. This allows the surgeon to maintain adequate surgical margins from the tumor lesion under the guidance of ICG-based NIR fluorescence imaging.[23] Be-

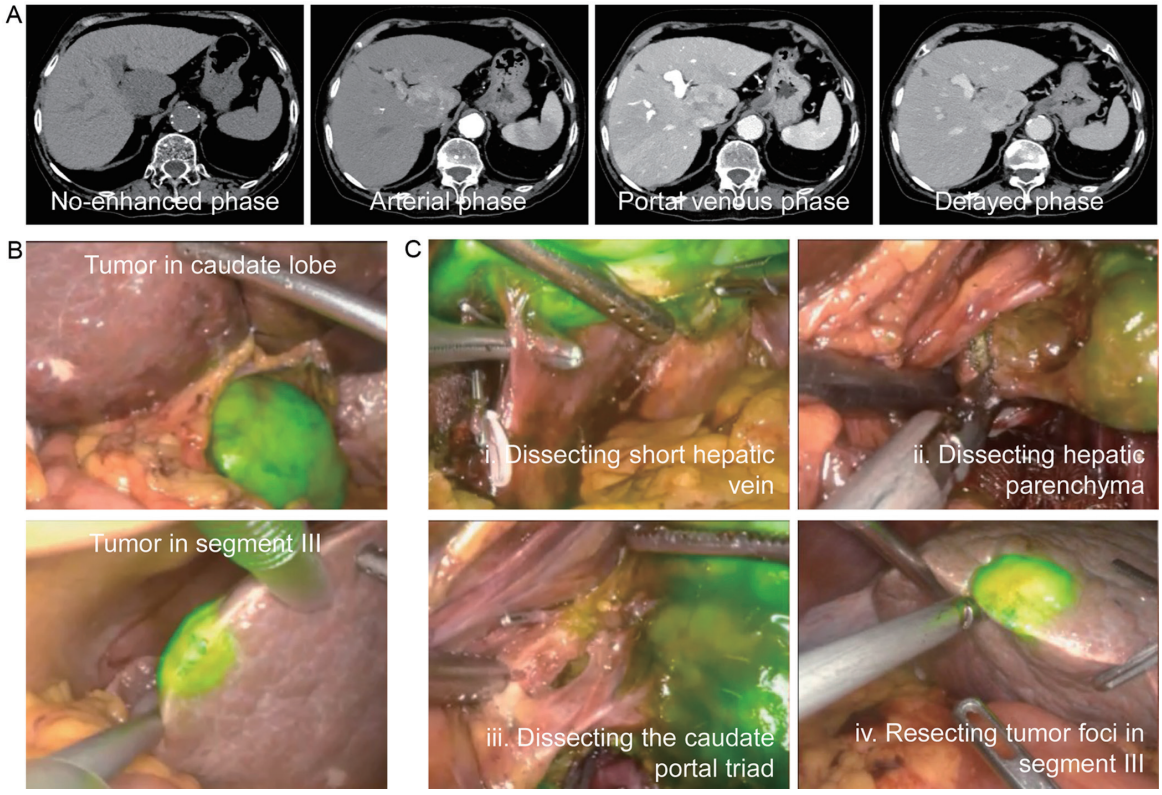

Fig. 1. A representative HCC patient performed ICG-based fluorescence-guided surgery. (A) Preoperative imaging of HCC lesion in caudate lobe by enhanced computed tomography scanning. (B) Fluorescence imaging of an HCC lesion in the caudate lobe and an accidental tumor lesion in segment III. (C) Real-time fluorescence imaging of tumor resection through ICG fluorescence guidance. HCC, Hepatocellular carcinoma; ICG, Indocyanine green.

sides, the suspected tumor nodule identified by preoperative imaging techniques can be intraoperatively diagnosed based on fluorescence imaging, potentially modifying the clinical stage of HCC. As illustrated in Figure 1A, the preoperative imaging using enhanced CT scanning demonstrates an HCC lesion measuring 7 cm × 5 cm located in the caudate lobe of the liver. During surgery, this lesion, along with another lesion, was identified and localized through the strong fluorescence signal from ICG accumulated in the tumor (Fig. 1B). According to the fluorescence guidance, the tumor boundaries were distinguished from the left pedicle of the liver, the inferior vena cava, and the papillary process of the caudate lobe, and then the tumor lesion was dissected along these boundaries (Fig. 1C). Additionally, due to the low uptake ability of ICG in poorly differentiated HCC tissues, the fluorescence signal provided by the lesion itself is usually weak. However, because of the compression of the tumor on normal liver tissue, the excretion of ICG is delayed, resulting in a characteristic ring-shaped fluorescence around the cancer tissue. Partial cells in moderately differentiated HCC tissues lose their uptake function, typically showing a partial fluorescence signal. Highly differentiated HCC tissues retain a specific uptake ability for ICG, but their bile excretion function is abnormal, leading to prolonged fluorescence display and a homogeneous fluorescence signal.[29] Based on these anatomical abnormalities and dysfunctions, HCC lesions can be distinguished from noncancerous nodules during surgery, as illustrated by the strong fluorescence emitted by the HCC lesion, while the necrotic lesion displays little to no fluorescence signal (Fig. 2).

In addition, for patients with unresectable HCC at the current stage, the primary treatment options include local ablation, chemotherapy, radiotherapy, and interventional embolization, with transcatheter arterial embolization (TACE) being the most widely employed in clinical medicine.[30] TACE involves dissolving chemotherapy drugs, for instance, doxorubicin or carboplatin in an embolic agent (commonly lipiodol) and injecting the mixture into the tumor's blood supply via the hepatic artery. This leads to significant tumor cytotoxicity, ischemia, and hypoxia, while simultaneously inhibiting the proliferation of tumor cells and killing them.[31] Compared to systemic chemotherapy, TACE significantly increases the drug concentration in HCC tissue and reduces the probability of systemic adverse events. Additionally, when ICG is added to the embolic agent, clinicians can observe changes in the tumor post-TACE treatment and facilitate intraoperative tumor navigation, leading to improved therapeutic effect. However, for unresectable HCC tumors larger than 10 cm in diameter, the therapeutic effects are often unsatisfactory. Common reasons include insufficient drug load, rapid drug clearance, and biotoxicity.[32]

In recent years, a research team developed a new super-stable homogeneous intermixed formulation technology to improve the stability of drugs in lipiodol (Fig. 3).[33] At a certain temperature and pressure, carbon dioxide is continuously injected into the reactor to make the fluid reach the supercritical stage above the critical temperature. Under these conditions, the team successfully mixes clinically available drugs with lipiodol, achieving uniform and stable dispersion of the drugs within the lipiodol.[33] With the help of this technology, ICG can be more effectively dispersed in lipiodol (lipiodol-ICG formulation). Assisted by interventional proce-

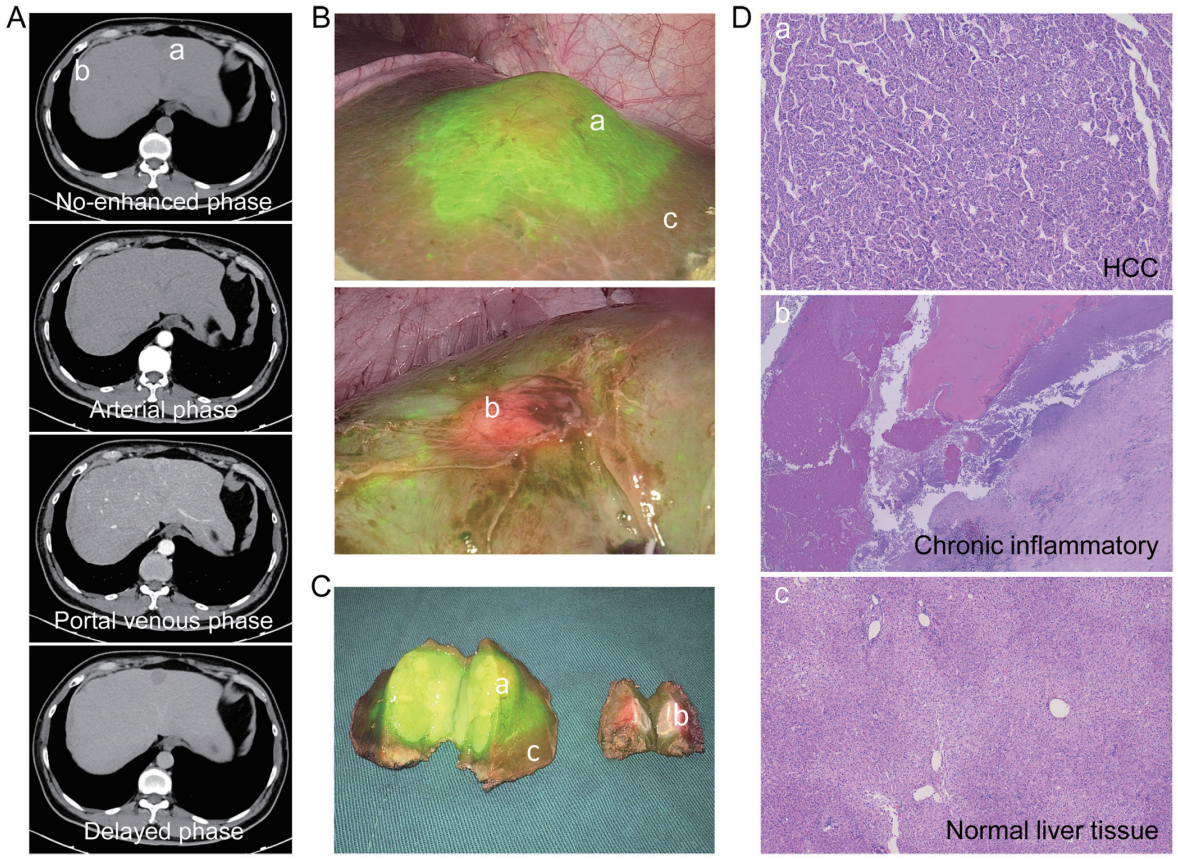

Fig. 2. A representative case of intraoperative identification of a HCC lesion and non-tumoral lesions using ICG-based fluorescence imaging. (A) Preoperative imaging of an HCC patient via enhanced computed tomography scanning. (B) Intraoperative ICG imaging. (C) *Ex vivo* fluorescence imaging of the HCC lesion and an abnormal nodule. (D) Postoperative pathological diagnosis of resected lesions. Magnification: ×40. HCC, Hepatocellular carcinoma; ICG, Indocyanine green.

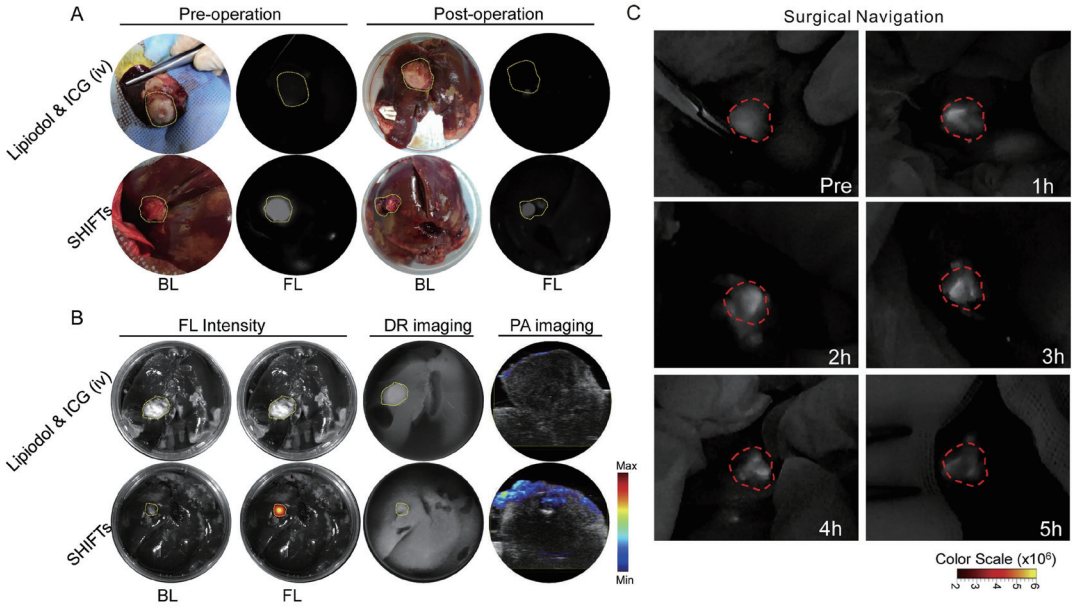

Fig. 3. Fluorescence-guided tumor resection in vivo after interventional treatment with super-stable homogeneous intermixed formulation technologies or normal lipiodol & ICG before surgery. (A) FL holographic projection and BL pre- and post-operation. (B) Fluorescence imaging, DR imaging and photoacoustic imaging of the resected tumors. (C) The anti-quenching effect over time under laser exposure.[33] (Reproduced with permission from Copyright 2020 Elsevier B.V.) ICG, Indocyanine green; BL, Bright light; FL, Fluorescence intensity; DR, Direct digital imaging; PA, Photoacoustic imaging.

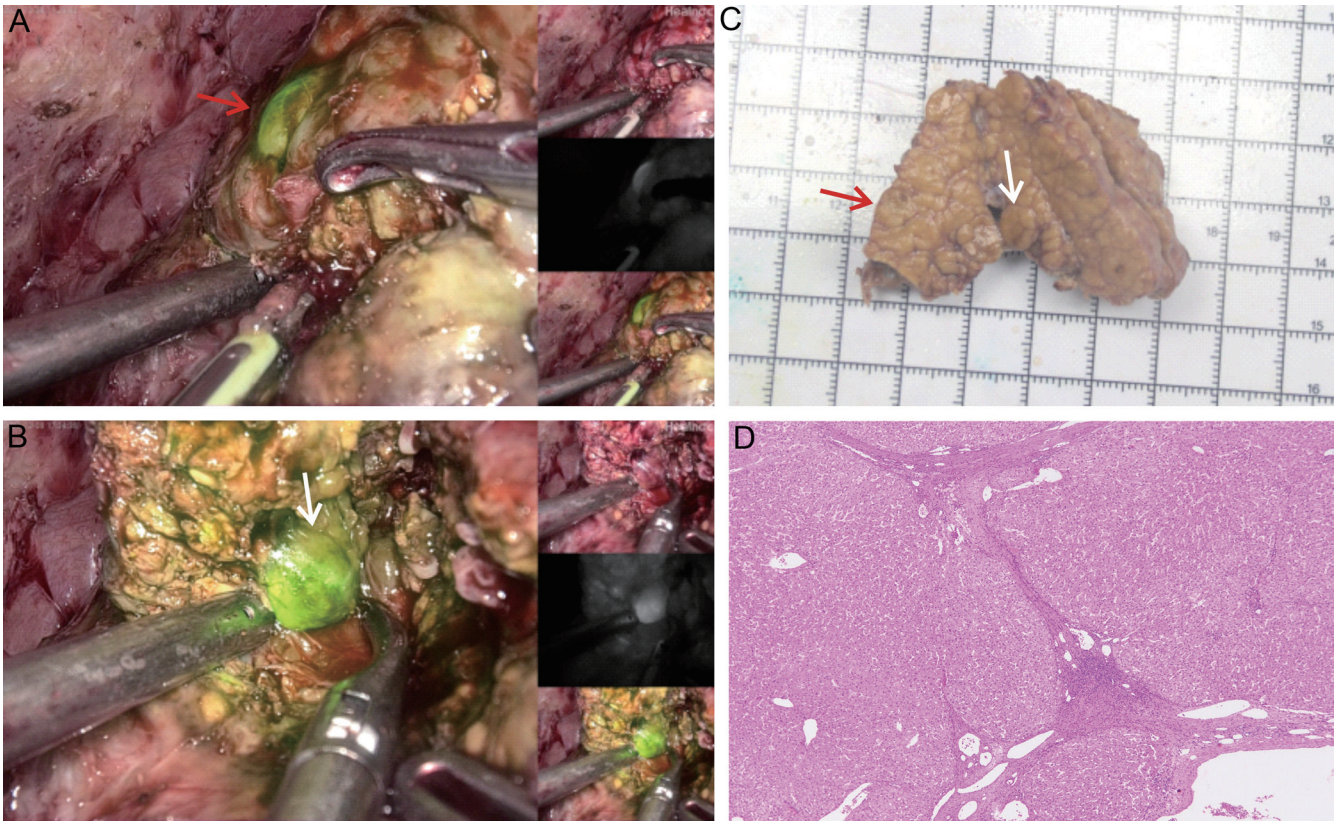

Fig. 4. Fluorescence imaging of false-positive nodules in liver cirrhosis after preoperative intravenous injection of indocyanine green. (A, B) Fluorescence imaging of liver nodules during liver tumor resection. (C) Gross specimen of resected liver tissue without neoplastic lesions. (D) Pathological examination confirmed liver cirrhosis. Magnification: ×40.

dures, the formulation is delivered to the local tumor region. Compared to free ICG of the same concentration, the fluorescence stability of the formulation is significantly improved. As a highly decentralized drug system, super-stable homogeneous intermixed formulation technology can overcome the aggregation effects that lead to fluorescence quenching.[34,35] This capability has been confirmed in both *in vitro* and *in vivo* experiments.[33] Another important point is the enhanced targeting for primary tumor tissues. The lipiodol-ICG formulation benefits from drug delivery *in situ* and the tumor cells' specific uptake of lipiodol, allowing for targeted delivery to tumor tissues. This will help the surgeon to remove the tumor tissue as completely as possible, helping to prevent tumor recurrence and metastasis.

Although ICG-based FGS has many advantages for HCC, there are still several areas for improvement in clinical practice, as follows: (i) ICG has limited detection ability for deep lesions. As the intensity of fluorescence decreases while passing through tissue, the proportion of light reaching the camera is greatly reduced. Thus, only surfaces or fluorescent structures less than 10 mm deep can be visualized.[36] (ii) ICG has poor tumor targeting ability and is completely passive. Its distribution in the liver is affected by blood flow and other physiological factors, such as the degree of cirrhosis, making it difficult to determine the optimal timing for preoperative administration.[37] If the degree of cirrhosis is severe and the administration time is too short, a large number of cirrhotic nodules will show fluorescence, as seen in Figure 4. (iii) Benign liver tumors also emit fluorescence due to ICG retention in tumor tissues because they lack bile ducts. Therefore, ICG fluorescence imaging cannot be used as a diagnostic method to distinguish between benign and malignant liver tumors. As shown in Figure 5, hepatic adenomas and focal nodular hyperplasia, verified by postoperative pathological examination, can also be illuminated following preoperative intravenous administration of ICG to assess liver function.

In conclusion, when using ICG for surgical navigation of HCC, surgeons need to consider the above factors and combine them with other imaging modalities and clinical findings to ensure the accuracy and safety of surgical navigation. Therefore, the development of innovative fluorescent probes for FGS of HCC with higher specificity, greater signal-to-noise ratio, and more convenient use has garnered significant attention in recent years to address the aforementioned deficiencies. In the following sections, we will summarize recent advances in this area.

Conventional fluorescent molecules for FGS of HCC

Under normal conditions, human cells and their microenvironment maintain a stable state at the molecular level. However, after HCC occurs, some biomolecules, including enzymes, reactive oxygen species (ROS), reactive sulfur species (RSS), pH, and other biomarkers, may fluctuate to a certain degree. These changes serve as specific targets that enable accurate monitoring of HCC.[38,39] Based on this, scientists have synthesized and verified a series of molecular fluorescent probes with better fidelity, high signal-to-noise ratio, and biological imaging specificity.

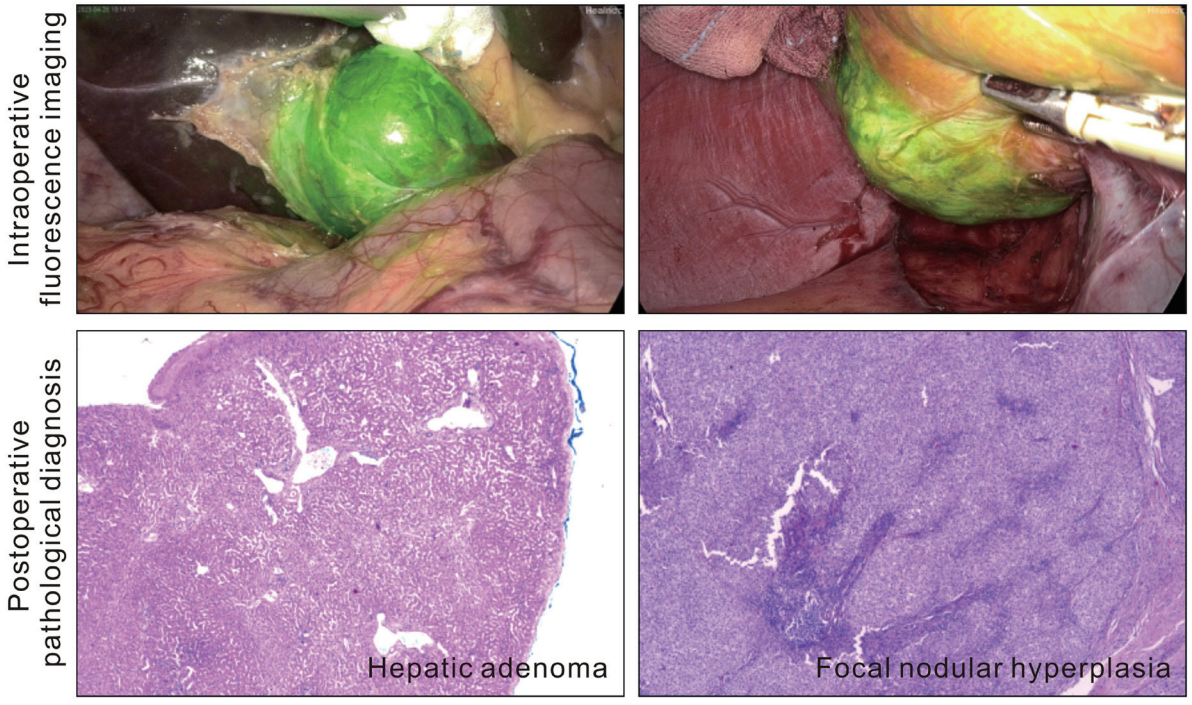

Fig. 5. Fluorescence imaging of benign liver tumors through preoperative intravenous injection of indocyanine green. Magnification: ×40.

Enzyme-responsive fluorescence imaging

Enzymes play a crucial role in maintaining the balance and stability of biological systems. Abnormal enzyme activity index is directly associated with the occurrence of various tumors, and can be used as a key index for clinical diagnosis and evaluation of specific diseases.[40] Over the past decade, significant progress has been made in fluorescent probes for detecting HCC overexpression enzymes. Here are several notable overexpressed enzymes and their corresponding molecular fluorescent probes.

Cyclooxygenase-2 (COX-2) is an enzyme typically absent in normal tissue but becomes activated and expressed when triggered by factors such as tumors or infections. Research has revealed that COX-2 plays a significant role in oncogenesis, proliferation, and migration in HCC.[41] Therefore, COX-2 may be the most suitable candidate target for fluorescence imaging of HCC. In 2017, Wang *et al*.[42] reported a COX-2-specific probe (COX-2 FP) and tested whether it could distinguish HCC both *in vitro* and *in vivo* (Fig. 6A). They determined the enhanced expression of COX-2 in human HCC cell lines (Fig. 6A-b). Fluorescence emission of COX-2 FP was then tested in HCC cell lines and a heterograft mouse model, showing that both could be clearly distinguished from normal liver cells or tissues based on the fluorescence signal (Fig. 6A-c, d). These results suggest that COX-2 FP could be a potential method to distinguish HCC, particularly in intraoperative imaging.

Histone deacetylases (HDACs) are a family of epigenetic enzymes that regulate gene expression, cell cycle progression, and apoptosis.[43] Consequently, they have emerged as an attractive target for novel cancer diagnostic and therapeutic strategies. In 2019, Tang *et al*. designed and synthesized an HDAC-targeted NIR probe, IRDye800CW-SAHA, for liver cancer imaging and FGS.[44] This probe has strong affinity for HDAC and good biocompatibility. *In vivo* and *ex vivo* fluorescence imaging, IRDye800CW-SAHA showed high specificity and sensitivity, and tumor fluorescence signals could still be seen after subcutaneous accumulation for up to 48 h. In image-guided surgical studies, liver tumors could be precisely resected under fluorescence guidance. These findings demonstrate that IRDye800CW-SAHA can detect HDAC expression levels in tumors, enabling targeted imaging of HCC and FGS, with potential for clinical translation.

β-glucuronidase (GLU) is a lysosomal glycosidase whose main function is to participate in the degradation of glucuronidoglycans containing glucuronic acid and is associated with various pathophysiological conditions in the body.[45] Additionally, the active expression of GLU is closely related to the invasion, apoptosis, metastasis and proliferation of tumor cells. Compared with normal hepatocytes, GLU activity was significantly enhanced when hepatocytes became cancerous.[46] In 2022, Wang *et al*.[47] reported a fluorescent probe, DCDNO2, for the real-time, precise detection of GLU (Fig. 6B). DCDNO2 exhibited excellent fluorescence characteristics, such as high specificity, rapid response, and good biocompatibility. As shown in Figure 6B-b, when DCDNO2 was added to HepG2 cells, a strong fluorescence signal was observed. After baicalin pretreatment, the red fluorescence in HepG2 cells decreased significantly. In addition, DCDNO2 can accurately assist and guide the surgical removal of tumors after local spraying of DCDNO2 in mouse models of liver cancer (Fig. 6B-c). Therefore, DCDNO2 plays an important role in assisting HCC surgical resection.

ROS-responsive fluorescence imaging

According to previous literature, liver cancer cells can produce more ROS than normal liver cells.[48] Hypochlorous acid (HClO) is one of the most essential ROS and a critical target in current probe synthesis research. It is generated with the assistance of myeloperoxidase, catalyzing the oxidation reaction of hydrogen peroxide and chloride ion in the biological system.[49] The high reactivity of endogenous HClO makes it a

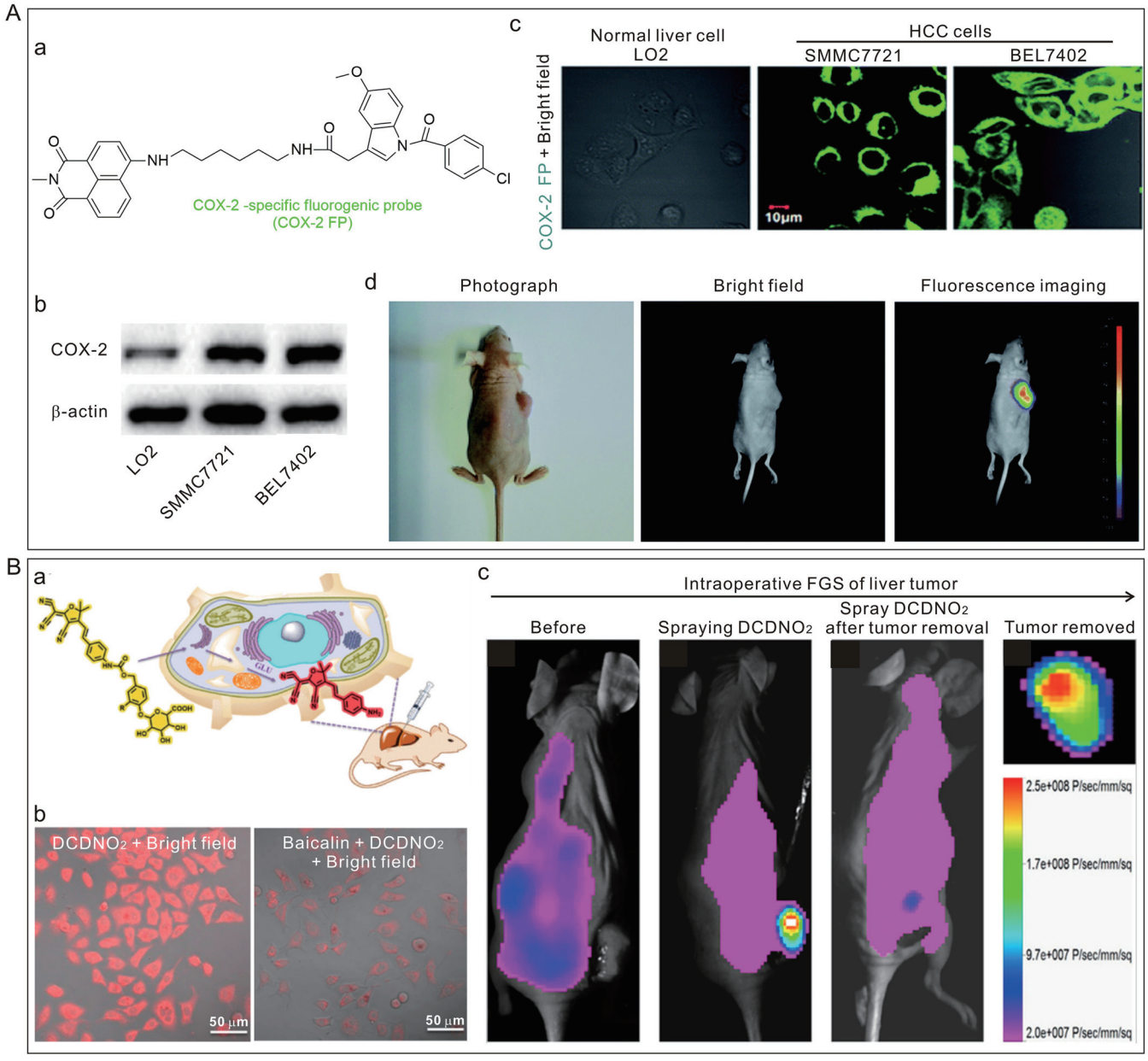

Fig. 6. Chemical structure and fluorescence images of enzyme-responsive probes for liver cancer *in vitro* and *in vivo*. (A) a. Molecular structure of COX-2 FP. b. COX-2 FP expression in LO2, SMMC7721, and BEL7402 cells by western blot assay. c. Fluorescence images of LO2, SMMC7721, and BEL7402 cells with COX-2 FP for 30 min. [COX-2 FP] = 5.0 μM. d. Fluorescence image of a xenograft tumor *in vivo* after intravenous injection of COX-2 FP for 30 min (30 μM, 50 μL).[42] (Copyright 2018 The Royal Society of Chemistry.) (B) a. Response mechanism of the probes DCDNO2 for β-Glucuronidase activity testing. b. Fluorescence image of DCDNO2 (10 μM) in HepG2 cells after 40 min of incubation (left image) and the fluorescence image of HepG2 cells after pretreatment with Baicalin (100 mM) for 30 m and with DCDNO2 (10 μM) for 40 min (right image). c. Fluorescence images after spraying DCDNO2 in mice bearing HepG2 xenograft tumors, mice with transplanted tumors removed, and resected tumors.[47] (Reproduced with permission from Copyright 2022 American Chemical Society.)

double-edged sword. On the one hand, it plays a key role in defending against invading pathogens; On the other hand, its abnormal accumulation can cause or aggravate various inflammation-related diseases.[50,51] Recent studies have shown that inflammatory injuries or diseases are major driving forces for cancer, and inflammatory signals may lead to carcinogenesis.[52,53] Therefore, tracking the level of HClO can be used to target liver cancer cells. Li *et al*.[54] designed and synthesized a near-infrared fluorescent probe (MBH-MT) (Fig. 7). The probe targets liver cells by transferring the melatonin fragment onto the methylene blue fluorophore (Fig. 7A). Four normal cells (HUVEC, LO2, RAW264.7, and HK-2) and one tumor cell (HepG2) were selected to evaluate whether probe MBH-MT can differentiate between normal and tumor cells. Tumor cells showed much higher fluorescence intensity than normal cells (Fig. 7B). *In vitro*, the fluorescent signal of HepG2 cell grafted tumors was significantly stronger than that of normal liver organs (Fig. 7C). Moreover, the probe successfully assisted liver tumor resection surgery in nude BALB/c mice with transplanted tumors (Fig. 7D, E). Based on

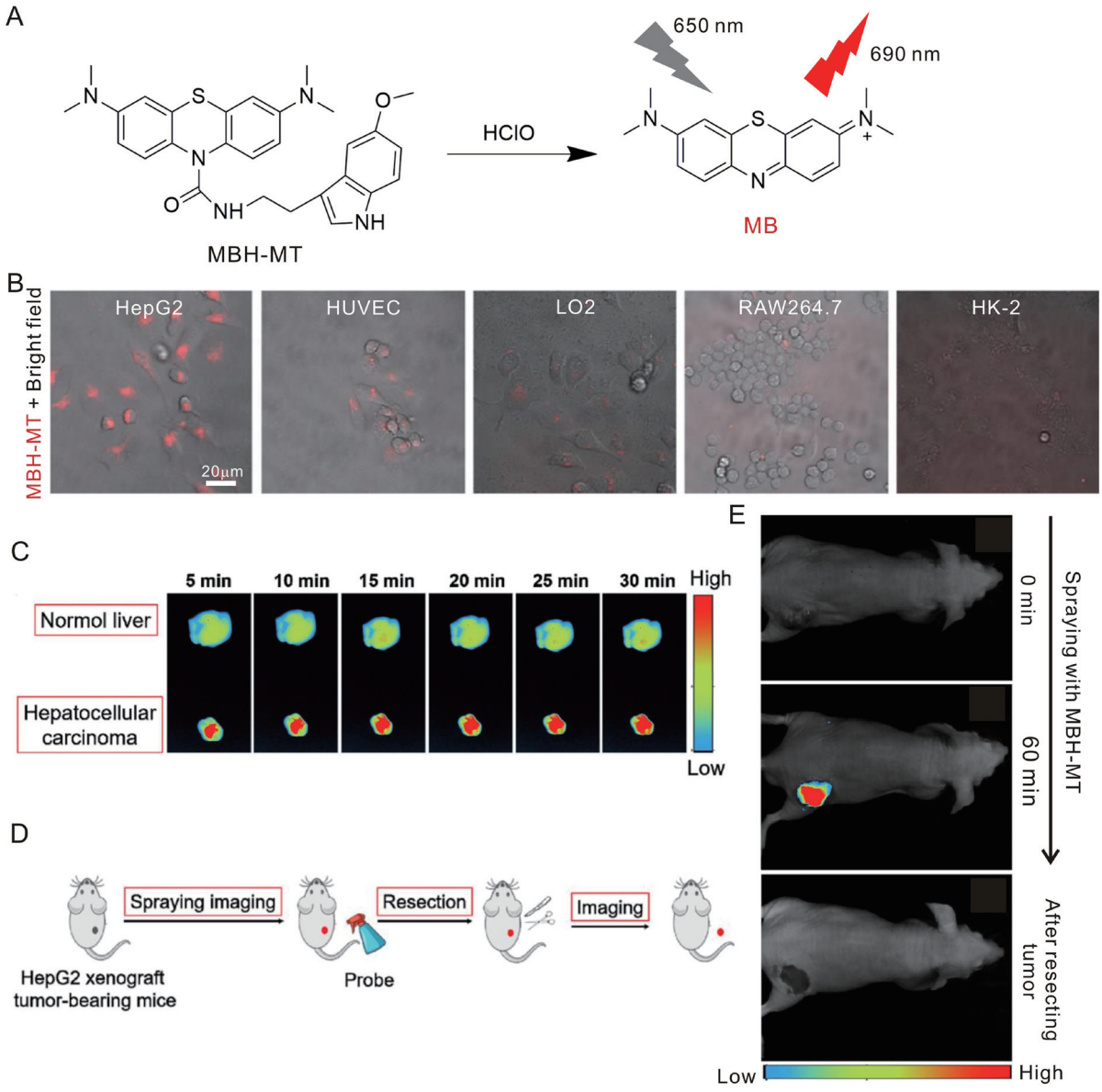

Fig. 7. Response mechanism and fluorescence images of MBH-MT and HClO in HepG2 cells and tumors. (A) Schematic diagram of probe MBH-MT response to hypochlorous acid. (B) Fluorescence images of probe MBH-MT (10 μM) for 30 min, followed by treatment with hypochlorous acid (25 μM) for another 15 min in HepG2, HUVEC, LO2, RAW264.7, and HK-2 cells. (C) Fluorescence images of normal mice and mice with hepatocellular tumors after incubation with MBH-MT (10 μM) for 5-30 min. (D) Surgical image-guided resection in HepG2 xenograft tumor-bearing mice. (E) Fluorescence images of HepG2 xenograft tumor-bearing mice intratumorally injected with probe MBH-MT (100 μM, 100 μL) at 0 min, 60 min, and after tumor resection.[54] (Reproduced with permission from Copyright 2023 Elsevier B.V.) MB, N-acetyl-5-methoxytryptamine; MBH-MT, A derivative of MB with near-infrared fluorescence.

the above results, the probe is expected to be an effective tool for HCC diagnosis and surgical treatment.

RSS-responsive fluorescence imaging

RSS mainly includes cysteine (Cys), homocysteine (Hcy), and glutathione (GSH), which have high reactivity and play irreplaceable roles in physiological and pathological processes.[55] They are also commonly used as scavengers of oxidants and are crucial for maintaining the redox state of biological systems.[56] Excessive RSS can trigger a series of related diseases such as inflammation, cancer, and Alzheimer's disease.[57]

In 2014, Ren *et al*.[58] developed a new ratiometric fluorescence probe for detecting GSH in a cancerous biomatrix (Fig. 8). The probe demonstrated high selectivity and sensitivity for detecting intracellular glutathione in four cancer cell lines (HepG2, Hep3B, Huh7, and HeLa) without causing cell toxicity (Fig. 8B). They constructed a quantitative model of intracellular GSH content using the probe ratio (B/Y). The probe was validated in the liver of normal mice, tumor xenografted mice, and tumor tissues of xenografted mice, with results as expected (Fig. 8C, D). The probe has the potential to be used as a highly sensitive and accurate biosensor for real-time intraoperative monitoring of HCC.

For targeting Cys, He *et al*.[59] designed a NIR fluorescent probe, Cy-Q. After Cy-Q was incubated with different ana-

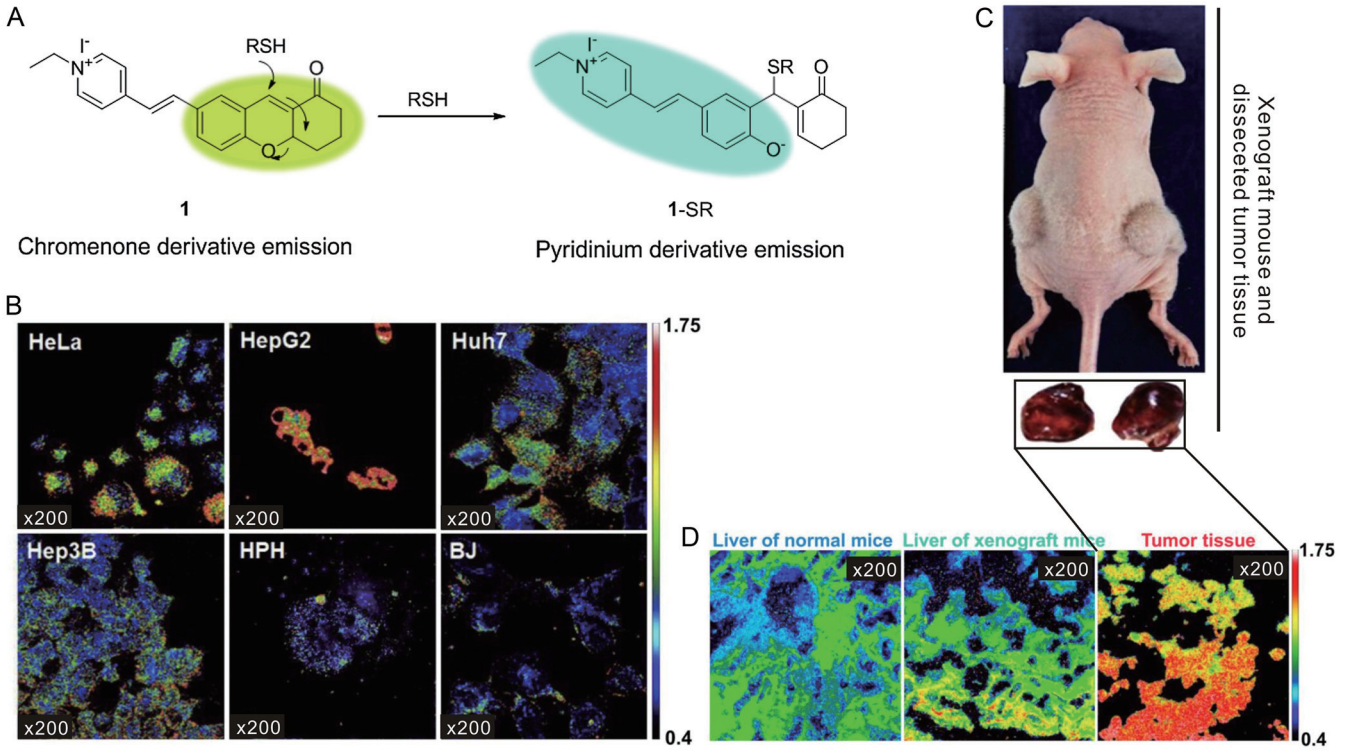

Fig. 8. Response mechanism and fluorescence images of RSH-responsive probe, for liver cancer *in vitro* and *in vivo* (A) Schematic diagram of probe 1 response to RSH. (B) Confocal fluorescence images of four carcinoma cell lines (HeLa, HepG2, Huh7, and Hep3B), HPH, and a normal fibroblast cell line (BJ) incubated with probe 1 (5 μM) for 2 h. Magnification: ×200. (C) Xenograft mouse model and dissected tumor tissue. (D) Confocal fluorescence images of the liver of normal mice, tumor xenograft mice, and tumor tissues of xenograft mice incubated with probe 1 (2 mM) for 2 h. Magnification: ×200.[58] (Reproduced with permission from Copyright 2014 Elsevier Ltd.) RSH, Intracellular reactive oxygen species oxidize protein sulfhydryl groups; SR, Sulfur group; HPH, Human primary hepatocytes.

lytes at 37°C for 2 h, a significant fluorescence increase was observed with the addition of Cys, Hcy, and GSH. At the same time, no obvious changes appeared with the other 16 analytes. The fluorescence intensity of Cys was twice as strong as the other two thiols, allowing effective differentiation of Cys from Hcy and GSH. Its level can be quantitatively monitored with specificity. The Cys fluorescence imaging of Cy-Q probe on normal mice, H22 tumor bearing mice and lipopolysaccharide (LPS) -induced mice was studied. The results showed that CY-Q probe preferently responded to liver tumor sites, which verified that the probe could easily distinguish liver tumor from normal tissue and inflammation. This work provides a promising NIR fluorescent probe with desired sensing properties for HCC imaging in biological systems.

Other fluorescent probes for HCC imaging

In addition to fluorescent probes activated by enzymes, ROS, and RSS, some probes are activated by other species, such as pH and polarity, which are also essential to living organisms. The pH value of the tumor microenvironment (6.2–6.9)[60] is slightly lower than the pH of the physiological microenvironment (7.2–7.4). This phenomenon is caused by the uncontrolled proliferation of cancer cells in the hypoxic environment.[61] Thus, precisely distinguishing subtle pH changes offers an ideal and practical way to differentiate cancer cells from normal cells. In 2019, Zhang *et al*.[62] developed a new dual-hepatocyte-targeted fluorescent probe (HPL-1). The molecule is "on" in the tumor microenvironment (pH 6.5) but "off" in the physiological microenvironment (pH 7.4). HPL-1 can distinguish HCC cells from other tissue cells and is the first example of small molecule fluorescent probes targeting pH changes in HCC cells. This heralds further possibilities for molecular fluorescent probe development in this area. Polarity is also a significant microenvironmental parameter, reflecting multiple complex biological processes, such as protein composition and signal transduction. It has been reported that polarity disorders are closely related to liver diseases.[63,64] In 2021, Lin *et al*.[65] developed a fluorescent probe ERNT for monitoring endoplasmic reticulum polarity. The probe can detect polarity changes during liver injury, including fatty liver, liver fibrosis, liver cirrhosis, and liver cancer, providing valuable insights into liver tumors and environmental polarity.

Additionally, ligand-modified fluorophores are another strategy to enhance the anchoring effect of fluorophores onto tumor cells. Integrin α6 is an adhesion molecule that exists on the cell surface and is involved in the process of cell attachment and tumor invasion and metastasis.[66] Evidence of overexpression of integrin α6 in approximately 94% of clinical early-stage HCC cases[67] suggests that it is a potential target for molecular fluorescence imaging in HCC assays. Feng *et al*.[68] previously identified a tumor-targeting peptide, CRWYDENAC (RWY), through phage display technology, confirming its high specificity and affinity for integrin α6. The researchers then labeled the RWY peptide with cyanine 7 (Cy7) to create a new molecular fluorescent probe, Cy7-RWY, targeting HCC.[69] The results showed that Cy7-RWY had high affinity to HCC-LM3 cells *in vitro*. By near infrared imaging, intravenous Cy7-RWY was only observed at the tumor site

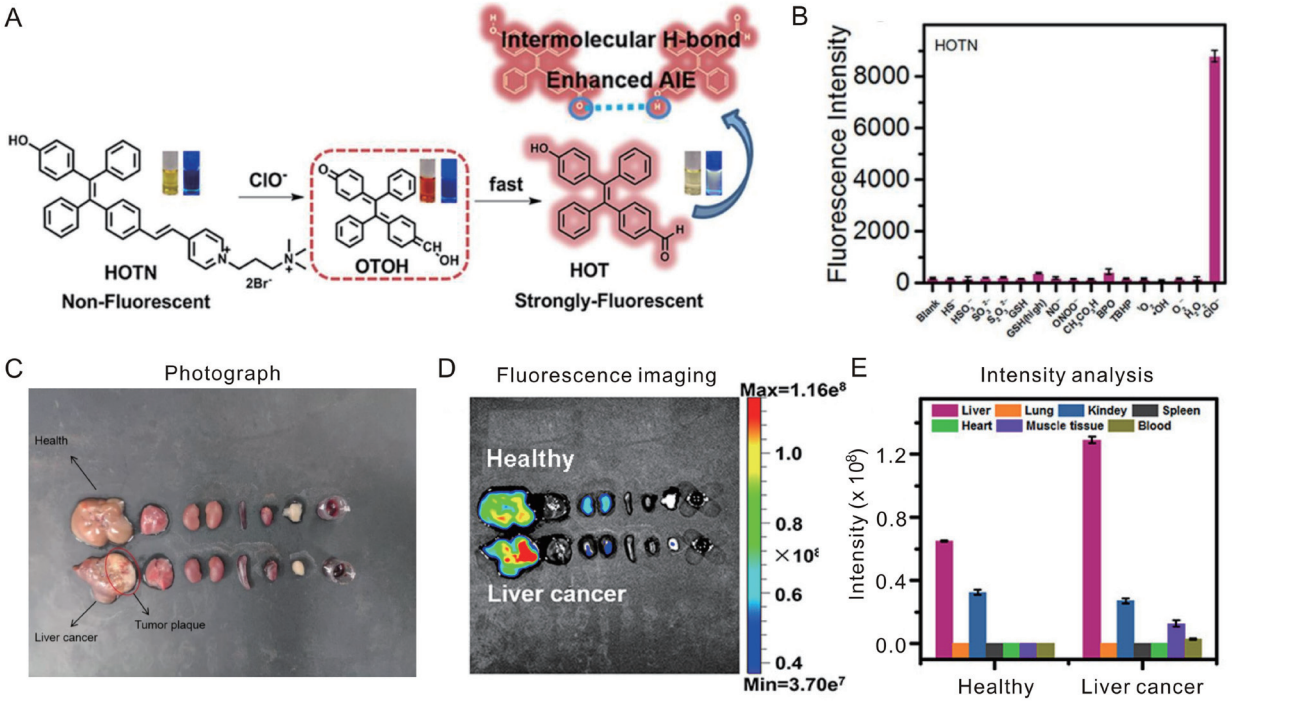

Fig. 9. Response mechanism and fluorescence imaging of AIE-active HOTN and ClO⁻ in liver cancer and normal tissues. (A) Response mechanism of probe HOTN's response to ClO⁻. (B) Fluorescence intensities of HOTN (10 μM) in PBS solution (pH = 7.4, 10 mM) in the presence of various interfering agents (50 μM). (C, D) Photographs and fluorescence imaging of heart, liver, spleen, lung, kidney tissue, and blood in healthy and liver cancer mice. (E) The fluorescence intensity of each part in Figure 9D.[95] (Reproduced with permission from Copyright 2020 American Chemical Society.) HOTN, OH−TPE−Py⁺−N⁺; OTOH, A intermediate products; HOT, OH−TPE−CHO; AIE, Aggregation-induced emission.

with a strong fluorescent signal in both subcutaneous HCCLM3 tumor models and HCC orthotopic transplantation tumor models. These findings indicate the specific targeting ability of Cy7-RWY for HCC tumors *in vivo*. Based on these validations, the Cy7-RWY probe may play a significant role in accurately delineating liver tumor lesions during future surgical resection of HCC.

Aggregation-induced emission luminogens (AIEgens)-based FGS for HCC

Although fluorescence molecular imaging has been widely used in simulated experiments for clinical image-guided surgery of liver tumors, its application in aqueous systems is greatly limited due to the aggregation-caused quenching (ACQ) effect. In high-concentration solutions or solid states, the formation of aggregates leads to close intermolecular contact, which alters the energy levels of electrons inside the molecules and disrupts the luminous pathway of the fluorescent compound. As a result, the amount of emitted light is reduced or even completely quenched. Additionally, the intensity of traditional fluorescent probes is affected by various factors, such as chemical reagents, ambient temperature, pH, and UV excitation light stability, which greatly reduce the accuracy and stability of detection and imaging. This limitation has driven the development of new fluorescent probes to achieve superior imaging capabilities.[70–75] Aggregation-induced emission (AIE) (including aggregation-enhanced emission (AEE)) has gained tremendous interest in research since its discovery in 2001.[76] Unlike conventional fluorophores that suffer from the ACQ effect, AIE fluorophores are not emissive in solution but become highly emissive in the aggregated or solid state due to the restriction of intramolecular motions.[77,78] The simple synthesis of AIE molecules and its remarkable fluorescence properties make it very popular in the fields of chemical sensors, biosensors, cell imaging, smart materials, and therapeutics.[79–91] After 20 years of design and development, AIE materials now exhibit strong photobleaching resistance, with luminescence increasing as the concentration rises.[92,93] Notably, light regulation of different emission bands has been achieved through flexible chemical modifications, and several near-infrared probes have been developed to produce high-resolution images in cell imaging and related bioimaging techniques.[94] These advantages make AIE probes highly suitable for the future diagnosis and guidance of liver cancer tumors.

AIEgens for HCC imaging

In 2020, Wang *et al*.[95] reported an aqueous-soluble AIE probe (HOTN) for detecting HClO (Fig. 9). Based on the excellent selectivity of HOTN for ClO− *in vitro* (Fig. 9B), HOTN has been successfully applied to imaging liver tumors *in situ*. The fluorescence intensity in liver of mice with liver cancer was obviously higher than that of healthy mice, and the fluorescence in cancer spot was the brightest (Fig. 9C–E), suggesting that HOTN could serve as a powerful tool for detecting HClO in HCC.

In the same year, We report that a novel AIE fluorescent probe hexaphenyl-1, 3-butadiene derivative (ZZ-HPB-NC) has a highly selective and immediate response to HCC.[96] In the frozen section of HCC, the fluorescence of ZZ-HPB-NC can be quickly lit by simple spraying, but there is no obvious fluorescence change in the liver cirrhosis, benign nodule tissue and normal liver tissue. Compared with the most authoritative hematoxylin and eosin staining, the detection

speed and accuracy of ZZ-HPB-NC are higher. The results showed that ZZ-HPB-NC staining provided experimental data basis for the intraoperative diagnosis of HCC, and had potential clinical application value. Based on the successful detection of liver tumor lesions using ZZ-HPB-NC, its isomer, all-trans configuration HPB-NC (EE-HPB-NC), was designed and synthesized.[97] Remarkably, EE-HPB-NC can identify normal liver tissue, and as an auxiliary tool, it can significantly improve the accuracy of ZZ-HPB-NC in identifying liver tumors (Fig. 10A).[97] In the HepG2/LO2 co-culture system, ZZ-HPB-NC and EE-HPB-NC can accurately label HepG2 and LO2 cells, respectively (Fig. 10B). Similarly, at the fresh tissue level, tumor lesions gradually fluoresce in ZZ-HPB-NC staining, reaching the maximum fluorescence intensity within 2 minutes, while normal liver tissues in the same dish remain unchanged. Moreover, EE-HPB-NC can also label normal tissues within 2 minutes (Fig. 10C). To effectively use HPB-NC for surgical navigation of solid hepatic tumors *in situ*, mouse orthotopic liver tumor models were established. Significant green fluorescence appeared in the tumor lesions with ZZ-HPB-NC staining, including tumors that had metastasized subcutaneously. EE-HPB-NC accurately labeled normal liver tissue to help guide complete tumor resection (Fig. 10D). These two probes complement each other to construct a configuration-induced cross-identification fluorescence imaging strategy, demonstrating their potential for clinical applications in real-time surgical fluorescence navigation.

Nanoprobes decorated with AIEgens as fluorophores for FGS of HCC

Although AIE probes have superior luminescence characteristics compared to traditional ACQ fluorescent dyes and can detect HCC lesion sites as described above, there is still a long way to go from laboratory research to clinical application. The main reason is that the complex *in vivo* environment presents a bottleneck in selecting drug delivery routes. For example, due to the complex distribution of tumors *in vivo*, imaging clearance is often difficult and may even be almost synchronized with the liver tumor, which affects the surgeon's judgment of tumor boundaries and can lead to surgical failure. Additionally, during the administration process, AIE probes may become unstable and degrade prematurely, which weakens the luminescence or causes nonspecific deposition in other tissues and organs, resulting in inaccurate imaging. Therefore, there is an urgent need to develop AIE probes with stronger targeting, more stability, and more convenient drug delivery for clinical applications. AIE nanoprobes, with their relatively stable core structure, stronger fluorescence, adjustable size, and modifiable outer layer, may meet this challenge.

α-fucosidase (AFU) is widely present in various tissues and cells, as a member of the glycosidase family, AFU can hydrolyze α-L-focusidase residues on lysosomes and their terminal glycolipids or glycoproteins.It is highly active within a pH range of 4−6.5.[98] Previous studies have shown that detecting overexpression of serum AFU levels diagnosed 85% of HCC patients six months earlier than ultrasonography.[99] Therefore, real-time detection of AFU could be a promising strategy for early diagnosis of HCC. In 2022, Situ *et al*.[100] constructed an AIE molecular fluorescent probe (α-Fuc-DCM), as shown in Figure 11. The probe was assembled from DCM-O^- and α-L-fucose residues. The authors confirmed that AFU effectively catalyzes the cleavage of α-L-fucose residues, thereby triggering fluorescence (Fig. 11A). Results from live cell imaging indicated that much brighter NIR fluorescence images were captured in HepG2 cells compared to HepG2 cells with an inhibitor and LO2 cells (Fig. 11B). In a mouse liver cancer model imaging experiment, α-Fuc-DCM allowed imaging of approximately 1 mm tumors. In comparison, after the subcutaneous injection of α-Fuc-DCM nanoparticles, there was minimal fluorescence(Fig. 11C, D), which also verified the specificity of the probe. Furthermore, immediately after killing the mice, fluorescence images of the tumor and other organs *in vitro* were recorded (Fig. 11E), confirming that the NIR fluorescent signal was emitted from the DCM-O– product. In conclusion, the authors established an effective method for monitoring AFU activity in vitro and in vivo, which could contribute to the early diagnosis and treatment of HCC.

γ-glutamyl transpeptidase (GGT) is a biological marker for the diagnosis of HCC and is the preferred reagent for early detection and intraoperative navigation.[101] In 2019, Liu *et al*.[102] designed and synthesized a novel NIR fluorescent nanoprobe (ABTT-Glu) with a coupled AIE effect and excited-state intramolecular proton transfer (ESIPT) effect for specific detection and imaging of GGT. This was the first demonstration of an "AIE + ESIPT" NIR nanoprobe for detecting GGT with high selectivity and sensitivity. The breakage of the γ-glutamyl bond catalyzed by GGT can alter the dispersed state of the probe and trigger both the AIE and ESIPT effects. ABTT-Glu has good specificity and sensitivity to GGT, and the detection time is short and the detection limit is low . The authors successfully imaged GGT activity in HepG2 cells and human liver tumor tissues with high specificity and long-term sustainability, meeting clinical needs and with great potential for precisely guiding human liver tumor surgery.

Multispectral optoacoustic tomography (MSOT) is a functional photoacoustic imaging method that works by irradiating a sample through multiple wavelengths and detecting ultrasonic signals from a light absorber. MSOT can produce three-dimensional (3D) images by capturing a stack of cross-sectional (chromatographic) images as a maximum intensity projection (MIP) image. In 2020, Zeng *et al*.[103] developed an activatable nanoprobe, BH-NO2@BSA, which responds explicitly to an overexpressed nitroreductase enzyme found in tumor cells and generates strong MSOT and NIR-I/NIR-II signals (Fig. 12A). The probe has been successfully used for *in vivo* fluorescence and MSOT imaging of subcutaneous liver tumors and liver tumors *in situ* (Fig. 12A-b), to guide preoperative precise localization of *in situ* liver tumors and accurate intraoperative identification of tumor margins (Fig. 12A-c), ensuring complete resection of liver tumors.

In the absence of oxygen, N-oxides can be converted into corresponding amines after binding with heme iron of various cytochrome P450 enzymes (CYP450), and irreversible two-electron reduction occurs. Interestingly, TPE-tetra(4-(diethylamino) phenyl)ethene (TPE-4NE) has shown AIE behavior and strong proton capture capability, which was inspired by Zhang *et al*. that TPE-4NE may be a promising candidate for deep tumor penetration.[104] In 2021, they synthesized an AIE nanoprobe (TPE-4NE-O),[105] which specifically turned on fluorescence in the presence of cytochrome P450 reductase (Fig. 12B-a). The probe can selectively illuminate hepatoma cells and show enhanced deep tumor penetration both *in vitro* and *in vivo* by charge conversion. After modification with FA-DSPE-PEG, FA-DSPE/TPE-4NE-O accumulated better within the tumor (Fig. 12B-b), enabling resection of micro tumors in Hepa1-6 tumor-bearing mice (Fig. 12B-c). More importantly, the probe exhibited good biocompatibility and negligible organ damage, without the risk of hemolysis. This simple yet promising probe provides new strategies for the visualization of minute liver tumors, showing great potential in HCC clinical surgery.

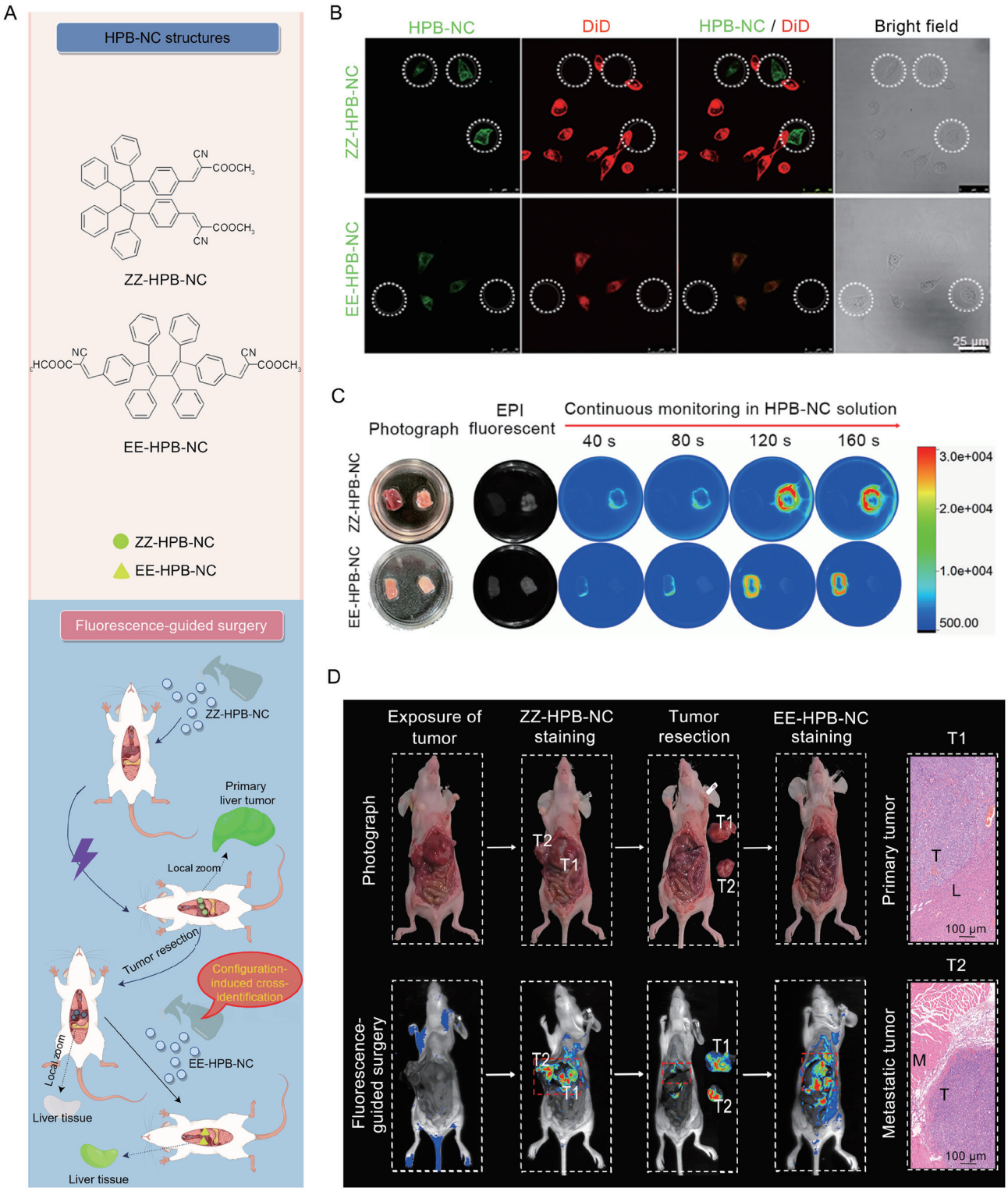

Fig. 10. Cis-trans isomerized HPB-NC molecules for configuration-induced cross-identification imaging and mouse liver tumor resection through fluorescence navigation. (A) Molecule structures of HPB-NC and schematic diagram of surgical navigation for liver tumors. (B) Fluorescence images of HPB-NC in the HepG2/LO2 cell co-culture system. LO2 cells were labeled with DiD, and HepG2 cells were highlighted by dotted circles. [HPB-NC] = 1 mM, [DiD] = 0.1 mM. (C) Real-time monitoring of fluorescence intensity changes in tumor lesions and normal liver tissues of mice *ex vivo*. Left: normal liver tissues; Right, tumor lesions. [HPB-NC] = 1 mM. (D) Fluorescence-guided resection of liver tumor and metastasis in an orthotopic model with HPB-NC. T, tumor tissue; L, liver normal tissue; M, muscle tissue. [HPB-NC] = 1 mM.[97] (Reproduced with permission from Copyright 2024 Aggregate published by SCUT, AIEI, and John Wiley & Sons Australia, Ltd.) ZZ-HPB-NC and EE-HPB-NC are hexaphenyl butadiene derivatives, which are cis-trans isomers of each other; DiD, Organelle commercial fluorescent dye.

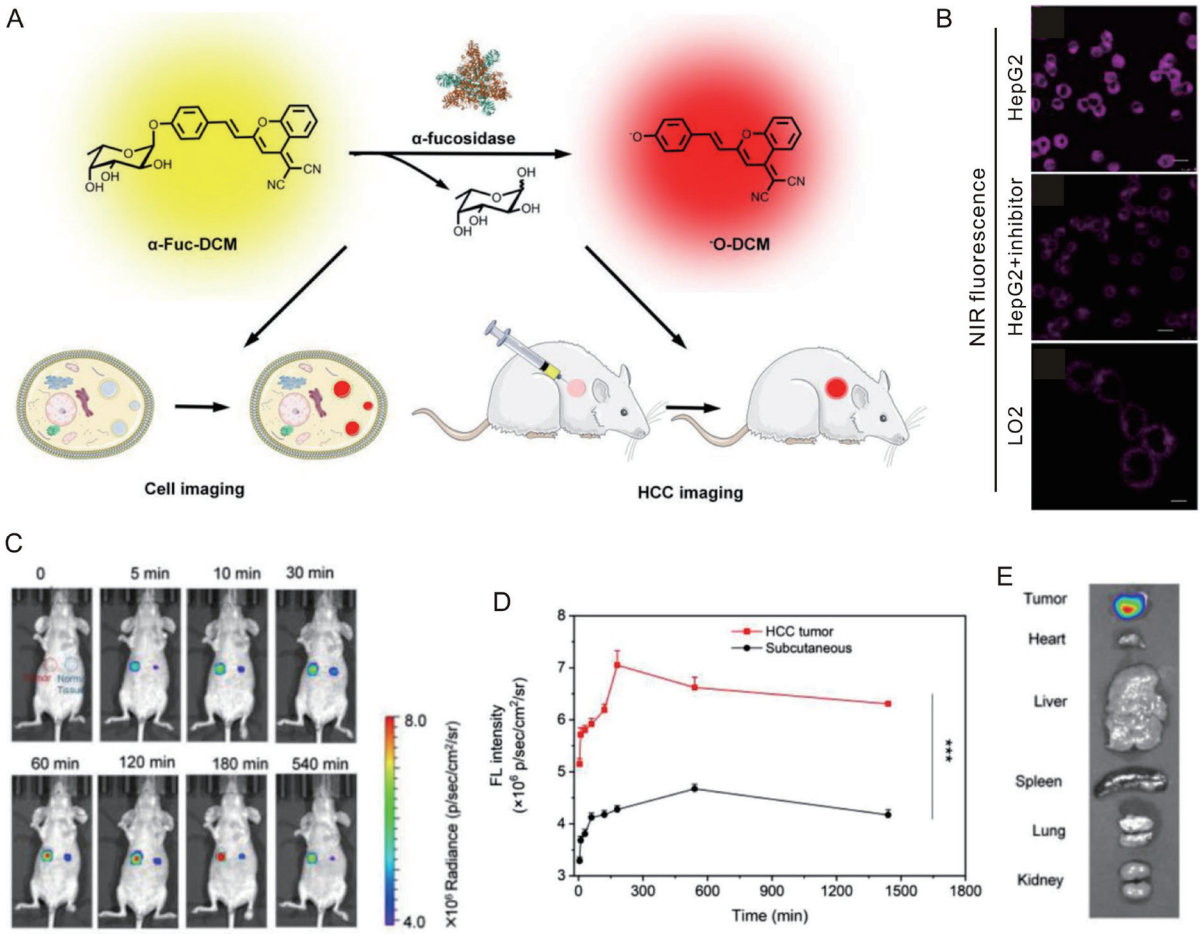

Fig. 11. Response mechanism and fluorescence imaging of α-fucosidase-responsive α-Fuc-DCM *in vitro* and *in vivo*. (A) Schematic diagram of probe α-Fuc-DCM response to AFU, and its specific detection in HCC tumor-bearing nude mice. (B) NIR fluorescence images of HepG2, HepG2 with inhibitor, and LO2 cell lines incubated with probe α-Fuc-DCM (10 μM) at 37°C for 2 h, imaging wavelength range from 605 to 725 nm, λ_{ex} = 560 nm. (C) NIR fluorescence imaging of HCC tumor and normal tissue in mice at 0–540 min following in situ injection of probe α-Fuc-DCM. (D) Plot of FL intensities of HCC tumor and normal tissue in Figure 10C. (E) Fluorescence images of the tumor and the main internal organs.[100] (Reproduced with permission from Copyright 2022 Aggregate published by SCUT, AIEI, and John Wiley & Sons Australia, Ltd.). DCM, A near-infrared fluorescent biosensor; HCC, Hepatocellular carcinoma.

Future perspective

Fluorescent probes are important tools for the visualization of physiopathological processes *in vivo*. In the past few years, significant progress has been made in developing fluorescent probes for guiding intraoperative resection of HCC. In this review, based on previous work, we systematically summarized the ICG widely used in clinical practice, molecular fluorescent probes targeted to identify biomarkers, including enzymes, ROS, RSS, etc., and the latest fluorescent probes based on the AIE effect. These probes showed excellent optical performance for the intraoperative real-time detection of simulated HCC.

Nevertheless, several key points remain to be addressed in the design of better fluorescent probes for the clinical transformation of HCC: (i) Optimize properties of fluorophores to enhance the tissue penetration depth of the detected signal. As is well-known, fluorophores in the NIR region have deeper tissue penetration than those in the visible region. Thus, the development of novel NIR fluorophores, especially in the NIR II region (1,000–1,700 nm), will provide a potential means to overcome tissue barriers. Besides, multimodal imaging, combining fluorescence signals with CT, MRI, photoacoustic imaging, etc., has also attracted attention as a means to achieve intraoperative visualization with higher resolution and deeper tissue penetration.[106] (ii) Improve the specific probe recognition to HCC to enhance the signal-to-noise ratio. Ligand-modified probes can increase the binding of probes to cancer cells and decrease distribution in normal tissue. As a result, tumor tissue emits strong fluorescence, while normal tissues show almost no fluorescence. On the other hand, "turn-on" fluorescence probes can light up tumor lesion when activated in the tumor microenvironment, but remain dark in normal tissues because they cannot be activated there. (iii) Develop new types of materials and technologies. For example, AIE technology can prevent probe quenching after aggregation, thereby improving fluorescence intensity. Additionally, AIE technology offers a novel strategy for highlighting tumor tissues through specific binding between AIEgens and specific biomacromolecules in tumor cells, triggering restriction of intramolecular motions to inducing emission. (iv) Explore new approaches for probe administration. The current mode of administration is usually intravenous injection, but some probes still distribute in normal tissues, resulting in undesired fluorescent signals. Therefore, a more effective approach would be to improve the accumulation of

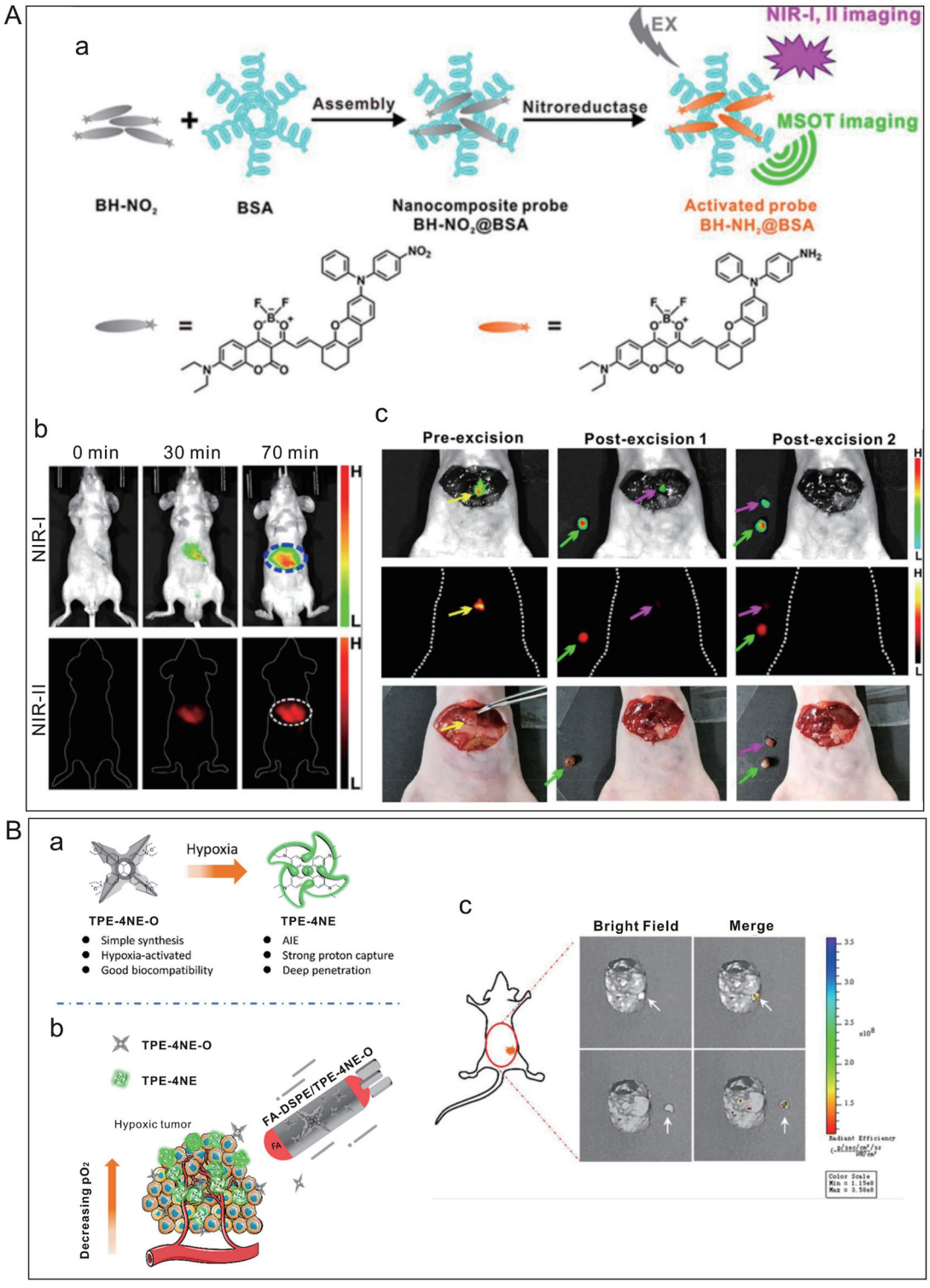

Fig. 12. Response mechanisms of probe BH-NO2@BSA and TPE-4NE-O, and intraoperative fluorescence navigation for orthotopic tumors. (A) a. Response mechanism of formation of probe BH-NO2@BSA and its response to nitroreductase. b. NIR-I and NIR-II fluorescence images of the same mouse with an orthotopic liver tumor at 0, 30, and 70 min with intravenous injection of BH-NO2@BSA. The blue or white dotted circle: the region of interest covering the whole orthotopic liver tumor. c. NIR-I (excitation filter 675 nm), NIR-II fluorescence images (excitation 808 nm), and white-light photographs of a mouse with exposed liver and fluorescence image-guided surgical resection of the orthotopic liver tumor (yellow arrow).[103] (Copyright 2020 American Chemical Society.) (B) a, b. Response mechanism of probe TPE-4NE-O and FA-DSPE/TPE-4NE-O response to the hypoxic tumor. c. Imaging-guided resection of tumors in Hepa1-6 bearing mice with FA-DSPE/TPE-4NE-O for 4 h.[105] (Reproduced with permission from Copyright 2020 American Chemical Society.). BSA, Bovine serum albumin; BH and TPE-4NE-O, Molecular probes; FA-DSPE, 1,2-distearoyl-sn-glycero-3-phosphoethanolamine-N-[folate].

fluorescent probes in tumor lesions, enhancing their distribution and retention. For example, nanocarriers can accurately deliver probes into tumor cells through the EPR effect and active targeting, where they accumulate and emit fluorescence. Additionally, a homogenous lipiodol-ICG formulation, developed using superstable homogeneous intermixed formulation technology for transcatheter arterial embolization, has been developed as an alternative administration method. This allows for local deposit in HCC tissue, enalbling the imaging of the full tumor region and boundaries in real-time and guiding laparoscopic hepatectomy.[107] (v) Design novel multifunctional probes for integrated diagnosis and treatment. For instance, fluorescent probe with photosensitivity can accurately destroy tumor lesions through photodynamic therapy while detecting them, or kill remaining tumor cells at the surgical margin during resection, improving the surgical treatment outcome.

Conclusions

Although several challenges remain, we firmly believe that with the continuous development of this field, fluorescent probes will provide new perspectives for clinical real-time navigation of HCC.

Acknowledgments

The authors thank Dr. Hongji Zhang for manuscript revision.

Funding

This work was financially supported by the National Natural Science Foundation of China (Grants 82170642, 82172754, 81874208, 22405079) and the Opening Project of Hubei Key Laboratory of Purification and Application of Plant Anti-cancer Active Ingredients (HLPAI2023001).

Conflict of interest

The authors have no conflict of interests related to this publication.

Author contributions

TX and DC were responsible for document collection, text writing and image processing; ZL was responsible for auxiliary image processing; LP, WP and YD were responsible for the guidance and revision of relevant theoretical knowledge; JZ and ML were responsible for the guidance and revision of the full text. All authors have approved the final version and publication of the manuscript.

References

[1] Forner A, Reig M, Bruix J. Hepatocellular carcinoma. Lancet 2018;391(10127):1301–1314. doi:10.1016/S0140-6736(18)30010-2, PMID:29307467.
[2] Siegel RL, Miller KD, Fuchs HE, Jemal A. Cancer statistics, 2022. CA Cancer J Clin 2022;72(1):7–33. doi:10.3322/caac.21708, PMID:35020204.
[3] You H, Wang F, Li T, Xu X, Sun Y, Nan Y, *et al*. Guidelines for the Prevention and Treatment of Chronic Hepatitis B (version 2022). J Clin Transl Hepatol 2023;11(6):1425–1442. doi:10.14218/JCTH.2023.00320, PMID:37719965.
[4] El-Serag HB. Epidemiology of viral hepatitis and hepatocellular carcinoma. Gastroenterology 2012;142(6):1264–1273.e1. doi:10.1053/j.gastro.2011.12.061, PMID:22537432.
[5] Sintusek P, Wanlapakorn N, Poovorawan Y. Strategies to Prevent Mother-to-child Transmission of Hepatitis B Virus. J Clin Transl Hepatol 2023;11(4):967–974. doi:10.14218/JCTH.2022.00332, PMID:37408824.
[6] Villanueva A. Hepatocellular Carcinoma. N Engl J Med 2019;380(15):1450–1462. doi:10.1056/NEJMra1713263, PMID:30970190.
[7] Fattovich G, Stroffolini T, Zagni I, Donato F. Hepatocellular carcinoma in cirrhosis: incidence and risk factors. Gastroenterology 2004;127(5 Suppl 1):S35–S50. doi:10.1053/j.gastro.2004.09.014, PMID:15508101.
[8] White DL, Kanwal F, El-Serag HB. Association between nonalcoholic fatty liver disease and risk for hepatocellular cancer, based on systematic review. Clin Gastroenterol Hepatol 2012;10(12):1342–1359.e2. doi:10.1016/j.cgh.2012.10.001, PMID:23041539.
[9] Calle EE, Rodriguez C, Walker-Thurmond K, Thun MJ. Overweight, obesity, and mortality from cancer in a prospectively studied cohort of U.S. adults. N Engl J Med 2003;348(17):1625–1638. doi:10.1056/NEJMoa021423, PMID:12711737.
[10] El-Serag HB, Hampel H, Javadi F. The association between diabetes and hepatocellular carcinoma: a systematic review of epidemiologic evidence. Clin Gastroenterol Hepatol 2006;4(3):369–380. doi:10.1016/j.cgh.2005.12.007, PMID:16527702.
[11] Brissot P, Pietrangelo A, Adams PC, de Graaff B, McLaren CE, Loréal O. Haemochromatosis. Nat Rev Dis Primers 2018;4:18016. doi:10.1038/nrdp.2018.16, PMID:29620054.
[12] Janicko M, Drazilova S, Jarcuska P. R0 Liver Resection should be a First-line Treatment for Selected Patients with Intermediate Hepatocellular Cancer. J Clin Transl Hepatol 2023;11(4):757–760. doi:10.14218/JCTH.2022.00123, PMID:37408800.
[13] Rosenthal EL, Warram JM, Bland KI, Zinn KR. The status of contemporary image-guided modalities in oncologic surgery. Ann Surg 2015;261(1):46–55. doi:10.1097/SLA.0000000000000622, PMID:25599326.
[14] Kokudo N, Takemura N, Ito K, Mihara F. The history of liver surgery: Achievements over the past 50 years. Ann Gastroenterol Surg 2020;4(2):109–117. doi:10.1002/ags3.12322, PMID:32258975.
[15] Machi J, Oishi AJ, Furumoto NL, Oishi RH. Intraoperative ultrasound. Surg Clin North Am 2004;84(4):1085–1111. doi:10.1016/j.suc.2004.04.001, PMID:15261754.
[16] Mieog JSD, Achterberg FB, Zlitni A, Hutteman M, Burggraaf J, Swijnenburg RJ, *et al*. Fundamentals and developments in fluorescence-guided cancer surgery. Nat Rev Clin Oncol 2022;19(1):9–22. doi:10.1038/s41571-021-00548-3, PMID:34493858.
[17] Nguyen QT, Tsien RY. Fluorescence-guided surgery with live molecular navigation—a new cutting edge. Nat Rev Cancer 2013;13(9):653–662. doi:10.1038/nrc3566, PMID:23924645.
[18] Low PS, Singhal S, Srinivasarao M. Fluorescence-guided surgery of cancer: applications, tools and perspectives. Curr Opin Chem Biol 2018;45:64–72. doi:10.1016/j.cbpa.2018.03.002, PMID:29579618.
[19] Zheng Y, Yang H, Wang H, Kang K, Zhang W, Ma G, *et al*. Fluorescence-guided surgery in cancer treatment: current status and future perspectives. Ann Transl Med 2019;7(Suppl 1):S6. doi:10.21037/atm.2019.01.26, PMID:31032287.
[20] Nakaseko Y, Ishizawa T, Saiura A. Fluorescence-guided surgery for liver tumors. J Surg Oncol 2018;118(2):324–331. doi:10.1002/jso.25128, PMID:30098296.
[21] Lwin TM, Hoffman RM, Bouvet M. Fluorescence-guided hepatobiliary surgery with long and short wavelength fluorophores. Hepatobiliary Surg Nutr 2020;9(5):615–639. doi:10.21037/hbsn.2019.09.13, PMID:33163512.
[22] Egloff-Juras C, Bezdetnaya L, Dolivet G, Lassalle HP. NIR fluorescence-guided tumor surgery: new strategies for the use of indocyanine green. Int J Nanomedicine 2019;14:7823–7838. doi:10.2147/IJN.S207486, PMID:31576126.
[23] Digital Medical Association of Chinese Medical Association; Digital Intelligent Surgery Professional Committee of Chinese Research Hospital Association; Liver Cancer Professional Committee of Chinese Medical Doctor Association; Clinical Precise Medicine Professional Committee of Chinese Medical Doctor Association; Medical Imaging and Equipment Professional Committee of China Graphics Society; Molecular Imaging Professional Committee of China Biophysical Society. [Guidelines for application of computer-assisted indocyanine green molecular fluorescence imaging in diagnosis and surgical navigation of liver tumors (2019)]. Nan Fang Yi Ke Da Xue Xue Bao 2019;39(10):1127–1140. doi:10.12122/j.issn.1673-4254.2019.10.01, PMID:31801707.
[24] Reinhart MB, Huntington CR, Blair LJ, Heniford BT, Augenstein VA. Indocyanine Green: Historical Context, Current Applications, and Future Considerations. Surg Innov 2016;23(2):166–175. doi:10.1177/1553350615604053, PMID:26359355.
[25] Ishizawa T, Masuda K, Urano Y, Kawaguchi Y, Satou S, Kaneko J, *et al*. Mechanistic background and clinical applications of indocyanine green fluorescence imaging of hepatocellular carcinoma. Ann Surg Oncol 2014;21(2):440–448. doi:10.1245/s10434-013-3360-4, PMID:24254203.
[26] Desmettre T, Devoisselle JM, Soulie-Begu S, Mordon S. [Fluorescence properties and metabolic features of indocyanine green (ICG)]. J Fr Ophtalmol 1999;22(9):1003–1016. PMID:10609179.
[27] Gao Y, Li M, Song ZF, Cui L, Wang BR, Lou XD, *et al*. Mechanism of dynamic near-infrared fluorescence cholangiography of extrahepatic bile ducts and applications in detecting bile duct injuries using indocyanine green in animal models. J Huazhong Univ Sci Technolog Med Sci 2017;37(1):44–50. doi:10.1007/s11596-017-1692-1, PMID:28224425.
[28] Miyata A, Ishizawa T, Tani K, Shimizu A, Kaneko J, Aoki T, *et al*. Reappraisal of a Dye-Staining Technique for Anatomic Hepatectomy by the Concomitant Use of Indocyanine Green Fluorescence Imaging. J Am Coll Surg 2015;221(2):e27–e36. doi:10.1016/j.jamcollsurg.2015.05.005, PMID:26206659.
[29] Lim C, Vibert E, Azoulay D, Salloum C, Ishizawa T, Yoshioka R, *et al*. Indocyanine green fluorescence imaging in the surgical management of liver cancers: current facts and future implications. J Visc Surg 2014;151(2):117–124. doi:10.1016/j.jviscsurg.2013.11.003, PMID:24461273.

[30] Sun HC, Zhou J, Wang Z, Liu X, Xie Q, Jia W, *et al*. Chinese expert consensus on conversion therapy for hepatocellular carcinoma (2021 edition). Hepatobiliary Surg Nutr 2022;11(2):227–252. doi:10.21037/hbsn-21-328, PMID:35464283.
[31] Wei ZQ, Zhang YW. Transcatheter arterial chemoembolization followed by surgical resection for hepatocellular carcinoma: a focus on its controversies and screening of patients most likely to benefit. Chin Med J (Engl) 2021;134(19):2275–2286. doi:10.1097/CM9.0000000000001767, PMID:34593696.
[32] Kishore SA, Bajwa R, Madoff DC. Embolotherapeutic Strategies for Hepatocellular Carcinoma: 2020 Update. Cancers (Basel) 2020;12(4):791. doi:10.3390/cancers12040791, PMID:32224882.
[33] Chen H, Cheng H, Dai Q, Cheng Y, Zhang Y, Li D, *et al*. A superstable homogeneous lipiodol-ICG formulation for locoregional hepatocellular carcinoma treatment. J Control Release 2020;323:635–643. doi:10.1016/j.jconrel.2020.04.021, PMID:32302761.
[34] Lajunen T, Nurmi R, Wilbie D, Ruoslahti T, Johansson NG, Korhonen O, *et al*. The effect of light sensitizer localization on the stability of indocyanine green liposomes. J Control Release 2018;284:213–223. doi:10.1016/j.jconrel.2018.06.029, PMID:29964133.
[35] Zhang Y, Cheng HW, Chen H, Xu PY, Ren E, Jiang YH, *et al*. A pure nanoICG-based homogeneous lipiodol formulation: toward precise surgical navigation of primary liver cancer after long-term transcatheter arterial embolization. Eur J Nucl Med Mol Imaging 2022;49(8):2605–2617. doi:10.1007/s00259-021-05654-z, PMID:34939176.
[36] Chen Z, Lin K, Liu J. Application of three-dimensional visualization in surgical operation for primary liver cancer. Lin Chuang Gan Dan Bing Za Zhi 2022;38(3):505–509. doi:10.3969/j.issn.1001-5256.2022.03.003.
[37] Ishizawa T, Fukushima N, Shibahara J, Masuda K, Tamura S, Aoki T, *et al*. Real-time identification of liver cancers by using indocyanine green fluorescent imaging. Cancer 2009;115(11):2491–2504. doi:10.1002/cncr.24291, PMID:19326450.
[38] Jayanthi VSPKSA, Das AB, Saxena U. Recent advances in biosensor development for the detection of cancer biomarkers. Biosens Bioelectron 2017;91:15–23. doi:10.1016/j.bios.2016.12.014, PMID:27984706.
[39] Wu L, Qu X. Cancer biomarker detection: recent achievements and challenges. Chem Soc Rev 2015;44(10):2963–2997. doi:10.1039/c4cs00370e, PMID:25739971.
[40] Li H, Kim D, Yao Q, Ge H, Chung J, Fan J, *et al*. Activity-Based NIR Enzyme Fluorescent Probes for the Diagnosis of Tumors and Image-Guided Surgery. Angew Chem Int Ed Engl 2021;60(32):17268–17289. doi:10.1002/anie.202009796, PMID:32939923.
[41] Misra S, Sharma K. COX-2 signaling and cancer: new players in old arena. Curr Drug Targets 2014;15(3):347–359. doi:10.2174/1389450115666140127102915, PMID:24467618.
[42] Wang H, Dong C, Jiang K, Zhang S, Long F, Zhang R, *et al*. Fluorescence imaging of hepatocellular carcinoma with a specific probe of COX-2. RSC Adv 2018;8(2):994–1000. doi:10.1039/c7ra07819f, PMID:35538969.
[43] Hesham HM, Lasheen DS, Abouzid KAM. Chimeric HDAC inhibitors: Comprehensive review on the HDAC-based strategies developed to combat cancer. Med Res Rev 2018;38(6):2058–2109. doi:10.1002/med.21505, PMID:29733427.
[44] Tang C, Du Y, Liang Q, Cheng Z, Tian J. Development of a Novel Histone Deacetylase-Targeted Near-Infrared Probe for Hepatocellular Carcinoma Imaging and Fluorescence Image-Guided Surgery. Mol Imaging Biol 2020;22(3):476–485. doi:10.1007/s11307-019-01389-4, PMID:31228075.
[45] Naz H, Islam A, Waheed A, Sly WS, Ahmad F, Hassan I. Human β-glucuronidase: structure, function, and application in enzyme replacement therapy. Rejuvenation Res 2013;16(5):352–363. doi:10.1089/rej.2013.1407, PMID:23777470.
[46] Basińska A, Floriańczyk B. Beta-glucuronidase in physiology and disease. Ann Univ Mariae Curie Sklodowska Med 2003;58(2):386–389. PMID:15323223.
[47] Wang J, Zhang L, Su Y, Qu Y, Cao Y, Qin W, *et al*. A Novel Fluorescent Probe Strategy Activated by β-Glucuronidase for Assisting Surgical Resection of Liver Cancer. Anal Chem 2022;94(19):7012–7020. doi:10.1021/acs.analchem.1c05635, PMID:35506678.
[48] Valko M, Leibfritz D, Moncol J, Cronin MT, Mazur M, Telser J. Free radicals and antioxidants in normal physiological functions and human disease. Int J Biochem Cell Biol 2007;39(1):44–84. doi:10.1016/j.biocel.2006.07.001, PMID:16978905.
[49] Winterbourn CC. Reconciling the chemistry and biology of reactive oxygen species. Nat Chem Biol 2008;4(5):278–286. doi:10.1038/nchembio.85, PMID:18421291.
[50] Jiao X, Li Y, Niu J, Xie X, Wang X, Tang B. Small-Molecule Fluorescent Probes for Imaging and Detection of Reactive Oxygen, Nitrogen, and Sulfur Species in Biological Systems. Anal Chem 2018;90(1):533–555. doi:10.1021/acs.analchem.7b04234, PMID:29056044.
[51] Mao Z, Ye M, Hu W, Ye X, Wang Y, Zhang H, *et al*. Design of a ratiometric two-photon probe for imaging of hypochlorous acid (HClO) in wounded tissues. Chem Sci 2018;9(28):6035–6040. doi:10.1039/c8sc01697f, PMID:30079216.
[52] Elinav E, Nowarski R, Thaiss CA, Hu B, Jin C, Flavell RA. Inflammation-induced cancer: crosstalk between tumours, immune cells and microorganisms. Nat Rev Cancer 2013;13(11):759–771. doi:10.1038/nrc3611, PMID:24154716.
[53] Prasad S, Gupta SC, Tyagi AK. Reactive oxygen species (ROS) and cancer: Role of antioxidative nutraceuticals. Cancer Lett 2017;387:95–105. doi:10.1016/j.canlet.2016.03.042, PMID:27037062.
[54] Li S, Wang P, Yang K, Liu Y, Cheng D, He L. Construction of HClO activated near-infrared fluorescent probe for imaging hepatocellular carcinoma. Anal Chim Acta 2023;1252:341009. doi:10.1016/j.aca.2023.341009, PMID:36935131.
[55] Giles GI, Jacob C. Reactive sulfur species: an emerging concept in oxidative stress. Biol Chem 2002;383(3-4):375–388. doi:10.1515/BC.2002.042, PMID:12033429.
[56] Lin VS, Chen W, Xian M, Chang CJ. Chemical probes for molecular imaging and detection of hydrogen sulfide and reactive sulfur species in biological systems. Chem Soc Rev 2015;44(14):4596–4618. doi:10.1039/c4cs00298a, PMID:25474627.
[57] Reja SI, Sharma N, Gupta M, Bajaj P, Bhalla V, Parihar RD, *et al*. A Highly Selective Fluorescent Probe for Detection of Hydrogen Sulfide in Living Systems: In Vitro and in Vivo Applications. Chemistry 2017;23(41):9872–9878. doi:10.1002/chem.201701124, PMID:28474839.
[58] Ren WX, Han J, Pradhan T, Lim JY, Lee JH, Lee J, *et al*. A fluorescent probe to detect thiol-containing amino acids in solid tumors. Biomaterials 2014;35(13):4157–4167. doi:10.1016/j.biomaterials.2014.01.055, PMID:24529899.
[59] He Q, Li R, Yuan Z, Kassaye H, Zheng J, Wei C, *et al*. A turn-on near-infrared fluorescent probe for detection of cysteine over glutathione and homocysteine in vivo. Anal Methods 2019;11(14):1857–1867. doi:10.1039/c8ay02792g.
[60] Zhang X, Lin Y, Gillies RJ. Tumor pH and its measurement. J Nucl Med 2010;51(8):1167–1170. doi:10.2967/jnumed.109.068981, PMID:20660380.
[61] Stubbs M, McSheehy PM, Griffiths JR, Bashford CL. Causes and consequences of tumour acidity and implications for treatment. Mol Med Today 2000;6(1):15–19. doi:10.1016/s1357-4310(99)01615-9, PMID:10637570.
[62] Zhang Y, Li Z, Ge H, Zhu X, Zhao Z, Qi Z-Q, *et al*. Dual hepatocyte-targeting fluorescent probe with high sensitivity to tumorous pH: Precise detection of hepatocellular carcinoma cells. Sensors Actuat B Chem 2019;285:584–589. doi:10.1016/j.snb.2019.01.103.
[63] Tu T, Budzinska MA, Maczurek AE, Cheng R, Di Bartolomeo A, Warner FJ, *et al*. Novel aspects of the liver microenvironment in hepatocellular carcinoma pathogenesis and development. Int J Mol Sci 2014;15(6):9422–9458. doi:10.3390/ijms15069422, PMID:24871369.
[64] Hernandez-Gea V, Toffanin S, Friedman SL, Llovet JM. Role of the microenvironment in the pathogenesis and treatment of hepatocellular carcinoma. Gastroenterology 2013;144(3):512–527. doi:10.1053/j.gastro.2013.01.002, PMID:23313965.
[65] Yin J, Quan W, Kong X, Liu C, Lu B, Lin W. Utilizing a Solvatochromic Optical Agent to Monitor the Polarity Changes in Dynamic Liver Injury Progression. ACS Appl Bio Mater 2021;4(4):3630–3638. doi:10.1021/acsabm.1c00130, PMID:35014449.
[66] Bon G, Folgiero V, Di Carlo S, Sacchi A, Falcioni R. Involvement of alpha6beta4 integrin in the mechanisms that regulate breast cancer progression. Breast Cancer Res 2007;9(1):203. doi:10.1186/bcr1651, PMID:17319974.
[67] Feng GK, Ye JC, Zhang WG, Mei Y, Zhou C, Xiao YT, *et al*. Integrin α6 targeted positron emission tomography imaging of hepatocellular carcinoma in mouse models. J Control Release 2019;310:11–21. doi:10.1016/j.jconrel.2019.08.003, PMID:31400382.
[68] Feng G-K, Zhang M-Q, Wang H-X, Cai J, Chen S-P, Wang Q, *et al*. Identification of an Integrin α6-Targeted Peptide for Nasopharyngeal Carcinoma-Specific Nanotherapeutics. Adv Therap 2019;2(7):1900018. doi:10.1002/adtp.201900018.
[69] Lin YZ, Wu Y, Cao DH, Peng YJ, Deng J, Lin WJ, *et al*. Integrin α6 Targeted Near Infrared Fluorescent Imaging and Photoacoustic Imaging of Hepatocellular Carcinoma in Mice. J Clin Transl Hepatol 2023;11(1):110–117. doi:10.14218/JCTH.2021.00414, PMID:36406330.
[70] Hong G, Antaris AL, Dai H. Near-infrared fluorophores for biomedical imaging. Nat Biomed Eng 2017;1(1):0010. doi:10.1038/s41551-016-0010.
[71] Li T, Liu L, Xu P, Yuan P, Tian Y, Cheng Q, *et al*. Multifunctional Nanotheranostic Agent for NIR-II Imaging-Guided Synergetic Photothermal/Photodynamic Therapy. Adv Therap 2021;4(3):2000240. doi:10.1002/adtp.202000240.
[72] Li X, Lovell JF, Yoon J, Chen X. Clinical development and potential of photothermal and photodynamic therapies for cancer. Nat Rev Clin Oncol 2020;17(11):657–674. doi:10.1038/s41571-020-0410-2, PMID:32699309.
[73] Younis MR, Wang C, An R, Wang S, Younis MA, Li ZQ, *et al*. Low Power Single Laser Activated Synergistic Cancer Phototherapy Using Photosensitizer Functionalized Dual Plasmonic Photothermal Nanoagents. ACS Nano 2019;13(2):2544–2557. doi:10.1021/acsnano.8b09552, PMID:30730695.
[74] Zhao J, Yan K, Xu G, Liu X, Zhao Q, Xu C, *et al*. An Iridium (III) Complex Bearing a Donor–Acceptor–Donor Type Ligand for NIR-Triggered Dual Phototherapy. Adv Funct Mater 2021;31(11):2008325. doi:10.1002/adfm.202008325.
[75] Zheng J, Liu Y, Song F, Jiao L, Wu Y, Peng X. A nitroreductase-activatable near-infrared theranostic photosensitizer for photodynamic therapy under mild hypoxia. Chem Commun (Camb) 2020;56(43):5819–5822. doi:10.1039/d0cc02019b, PMID:32329480.
[76] Luo J, Xie Z, Lam JW, Cheng L, Chen H, Qiu C, *et al*. Aggregation-induced emission of 1-methyl-1,2,3,4,5-pentaphenylsilole. Chem Commun (Camb) 2001;(18):1740–1741. doi:10.1039/b105159h, PMID:12240292.
[77] Wang H, Li Q, Alam P, Bai H, Bhalla V, Bryce MR, *et al*. Aggregation-Induced Emission (AIE), Life and Health. ACS Nano 2023;17(15):14347–14405. doi:10.1021/acsnano.3c03925, PMID:37486125.
[78] Peng Q, Shuai Z. Molecular mechanism of aggregation-induced emission. Aggregate 2021;2(5):e91. doi:10.1002/agt2.91.
[79] Li M, Gao Y, Yuan Y, Wu Y, Song Z, Tang BZ, *et al*. One-Step Formulation of

Targeted Aggregation-Induced Emission Dots for Image-Guided Photodynamic Therapy of Cholangiocarcinoma. ACS Nano 2017;11(4):3922–3932. doi:10.1021/acsnano.7b00312, PMID:28383899.
[80] Gao M, Tang BZ. Aggregation-induced emission probes for cancer theranostics. Drug Discov Today 2017;22(9):1288–1294. doi:10.1016/j.drudis.2017.07.004, PMID:28713054.
[81] Feng G, Liu B. Aggregation-Induced Emission (AIE) Dots: Emerging Theranostic Nanolights. Acc Chem Res 2018;51(6):1404–1414. doi:10.1021/acs.accounts.8b00060, PMID:29733571.
[82] Gao Y, Zheng QC, Xu S, Yuan Y, Cheng X, Jiang S, *et al*. Theranostic Nanodots with Aggregation-Induced Emission Characteristic for Targeted and Image-Guided Photodynamic Therapy of Hepatocellular Carcinoma. Theranostics 2019;9(5):1264–1279. doi:10.7150/thno.29101, PMID:30867829.
[83] Dai J, Wu X, Ding S, Lou X, Xia F, Wang S, *et al*. Aggregation-Induced Emission Photosensitizers: From Molecular Design to Photodynamic Therapy. J Med Chem 2020;63(5):1996–2012. doi:10.1021/acs.jmedchem.9b02014, PMID:32039596.
[84] Zhou T, Zhu J, Shang D, Chai C, Li Y, Sun H, *et al*. Mitochondria-anchoring and AIE-active photosensitizer for self-monitored cholangiocarcinoma therapy. Mater Chem Front 2020;4(11):3201–3208. doi:10.1039/D0QM00503G.
[85] Kang M, Zhang Z, Song N, Li M, Sun P, Chen X, *et al*. Aggregation-enhanced theranostics: AIE sparkles in biomedical field. Aggregate 2020;1(1):80–106. doi:10.1002/agt2.7.
[86] Chai C, Zhou T, Zhu J, Tang Y, Xiong J, Min X, *et al*. Multiple Light-Activated Photodynamic Therapy of Tetraphenylethylene Derivative with AIE Characteristics for Hepatocellular Carcinoma via Dual-Organelles Targeting. Pharmaceutics 2022;14(2):459. doi:10.3390/pharmaceutics14020459, PMID:35214196.
[87] Dai J, Xue H, Chen D, Lou X, Xia F, Wang S. Aggregation-induced emission luminogens for assisted cancer surgery. Coord Chem Rev 2022;464:214552. doi:10.1016/j.ccr.2022.214552.
[88] Wang F, Ho P-Y, Kam C, Yang Q, Liu J, Wang W, *et al*. An AIE-active probe for efficient detection and high-throughput identification of outer membrane vesicles. Aggregate 2023;4(4):e312. doi:10.1002/agt2.312.
[89] Li H, Zhang T, Liao Y, Liu C, He Y, Wang Y, *et al*. Recent advances of aggregation-induced emission in body surface organs. Aggregate 2024;5(2):e470. doi:10.1002/agt2.470.
[90] Jia J, Ma Z, Zhuang J, Huo L, Zhou C, Li N, *et al*. Lipid droplet-targeted NIR AIE photosensitizer evoking concurrent ferroptosis and apoptosis. Aggregate 2024;5(3):e516. doi:10.1002/agt2.516.
[91] Xu H, Chen X, Wang H, Wang C, Guo Y, Lin Y, *et al*. Utilization of aggregation-induced emission materials in urinary system diseases. Aggregate 2024;5(5):e580. doi:10.1002/agt2.580.
[92] Würthner F. Aggregation-Induced Emission (AIE): A Historical Perspective. Angew Chem Int Ed Engl 2020;59(34):14192–14196. doi:10.1002/anie.202007525, PMID:32662175.
[93] Zhu J, Jiang X. How does aggregation-induced emission aggregate interdisciplinary research? Aggregate 2024;5(2):e451. doi:10.1002/agt2.451.
[94] Giel M-C, Hong Y. Click chemistry in the design of AIEgens for biosensing and bioimaging. Aggregate 2023;4(4):e336. doi:10.1002/agt2.336.
[95] Han X, Ma Y, Chen Y, Wang X, Wang Z. Enhancement of the Aggregation-Induced Emission by Hydrogen Bond for Visualizing Hypochlorous Acid in an Inflammation Model and a Hepatocellular Carcinoma Model. Anal Chem 2020;92(3):2830–2838. doi:10.1021/acs.analchem.9b05347, PMID:31913021.
[96] Chen DD, Mao HL, Hong YN, Tang Y, Zhang Y, Li M, *et al*. Hexaphenyl-1,3-butadiene derivative: a novel "turn-on" rapid fluorescent probe for intraoperative pathological diagnosis of hepatocellular carcinoma. Mater Chem Front 2020;4(9):2716–2722. doi:10.1039/d0qm00262c.
[97] Chen D, Xiao T, Wang L, Chen S, Kam C, Zeng G, *et al*. A simple "spraying" fluorescence-guided surgery by AIE probes for liver tumor resection through configuration-induced cross-identification. Aggregate 2024;5(6):e550. doi:10.1002/agt2.550.
[98] Li C, Qian J, Lin JS. Purification and characterization of alpha-L-fucosidase from human primary hepatocarcinoma tissue. World J Gastroenterol 2006;12(23):3770–3775. doi:10.3748/wjg.v12.i23.3770, PMID:16773698.
[99] Mintz K, Waidely E, Zhou Y, Peng Z, Al-Youbi AO, Bashammakh AS, *et al*. Carbon dots and gold nanoparticles based immunoassay for detection of alpha-L-fucosidase. Anal Chim Acta 2018;1041:114–121. doi:10.1016/j.aca.2018.08.055, PMID:30340683.
[100] Zhang GQ, Feng W, Gao Z, Zhang GL, Wu X, Xiao Y, *et al*. A NIR ratiometric fluorescent biosensor for sensitive detection and imaging of α-L-fucosidase in living cells and HCC tumor-bearing mice. Aggregate 2022;4(2):e286. doi:10.1002/agt2.286.
[101] Miyata Y, Ishizawa T, Kamiya M, Yamashita S, Hasegawa K, Ushiku A, *et al*. Intraoperative imaging of hepatic cancers using γ-glutamyltranspeptidase-specific fluorophore enabling real-time identification and estimation of recurrence. Sci Rep 2017;7(1):3542. doi:10.1038/s41598-017-03760-3, PMID:28615696.
[102] Liu Y, Feng B, Cao X, Tang G, Liu H, Chen F, *et al*. A novel "AIE + ESIPT" near-infrared nanoprobe for the imaging of γ-glutamyl transpeptidase in living cells and the application in precision medicine. Analyst 2019;144(17):5136–5142. doi:10.1039/c9an00773c, PMID:31338492.
[103] Zeng Z, Ouyang J, Sun L, Zeng C, Zeng F, Wu S. Activatable Nanocomposite Probe for Preoperative Location and Intraoperative Navigation for Orthotopic Hepatic Tumor Resection via MSOT and Aggregation-Induced Near-IR-I/II Fluorescence Imaging. Anal Chem 2020;92(13):9257–9264. doi:10.1021/acs.analchem.0c01596, PMID:32530263.
[104] Wang Z, Nie H, Yu Z, Qin A, Zhao Z, Tang BZ. Multiple stimuli-responsive and reversible fluorescence switches based on a diethylamino-functionalized tetraphenylethene. J Mater Chem C 2015;3(35):9103–9111. doi:10.1039/C5TC02069G.
[105] Zhang Z, Wang R, Huang X, Zhu W, He Y, Liu W, *et al*. A Simple Aggregation-Induced Emission Nanoprobe with Deep Tumor Penetration for Hypoxia Detection and Imaging-Guided Surgery in Vivo. Anal Chem 2021;93(3):1627–1635. doi:10.1021/acs.analchem.0c04101, PMID:33377760.
[106] Wang C, Fan W, Zhang Z, Wen Y, Xiong L, Chen X. Advanced Nanotechnology Leading the Way to Multimodal Imaging-Guided Precision Surgical Therapy. Adv Mater 2019;31(49):e1904329. doi:10.1002/adma.201904329, PMID:31538379.
[107] Xiong Y, He P, Zhang Y, Chen H, Peng Y, He P, *et al*. Superstable homogeneous lipiodol-ICG formulation: initial feasibility and first-in-human clinical application for ruptured hepatocellular carcinoma. Regen Biomater 2023;10:rbac106. doi:10.1093/rb/rbac106, PMID:36683740.